2015

Development of an in-field voltammetric method for the determination of barium

Samantha N. Ridgway
Edith Cowan University

Edith Cowan University

Copyright Warning

Development of an in-field voltammetric method for the determination of barium

Bachelor of Science (Applied and Analytical Chemistry)
Honours
School of Natural Sciences
Faculty of Health, Engineering and Science
Edith Cowan University

Samantha Ridgway
Supervisors: Dr. Magdalena Wajrak & A/Prof. Mary Boyce
9th November, 2015

USE OF THESIS

This copy is the property of Edith Cowan University. However the literary rights of the author must also be respected. If any passage from this thesis is quoted or closely paraphrased in a paper or written work prepared by the user, the source of the passage must be acknowledged in the work. If the user desires to publish a paper or written work containing passages copied or closely paraphrased from this thesis, which passages would in total constitute an infringing copy for the purpose of Copyright Act, he or she must first obtain the written permission of the author to do so.

DECLARATION

I certify that thesis does not, to the best of my knowledge and belief:

(i) Incorporate without acknowledgement any material previously submitted for a degree or diploma in any institution of higher education;

(ii) Contain any material previously published or written by another person except where due credit is made in the text; or

(iii) Contain any defamatory material.

Signed:

Date:

ABSTRACT

This work presents a reliable, cost-effective, rapid and infield voltammetric method for the detection of barium. The optimized method consists of an ultrathin mercury film deposited *in-situ* on a glassy carbon electrode in 0.02 M potassium chloride without deoxygenation; a deposition potential of -2500 mV, pulse height = 50 mV, step duration = 10 ms and a scan rate of 100 mV/s using differential pulse anodic stripping voltammetry (DP-ASV).

The linear working range for barium was determined to be 5 – 80 µg/L (r^2 = 0.997), and limit of detection (LOD) was 1.6 µg/L, for 30 sec deposition time. Percent relative standard deviation for 10 measurements performed at 20 µg/L was 5.8%.

Application of the method allowed for the quantitative determination of barium concentration in a variety of waters, brake pad dust and gunshot residue (GSR) samples. Comparative analysis of sample results from DP-ASV with inductively-coupled plasma mass spectroscopy (ICP-MS) showed a mean percent difference of 1.8%. The method also permitted the simultaneous measurement of barium and lead, crucial for GSR samples.

ACKNOWLEDGMENTS

Much gratitude goes to my Honours supervisors, Dr. Magdalena Wajrak and A/Prof. Mary Boyce without whose guidance I would not have been able to complete this project. The proposal was ambitious but their enthusiasm, motivation and knowledge was the support I needed to persist despite dubious prospects. Dr. Wajrak's continued encouragement and advice whilst allowing me the space to experiment, was instrumental in achieving the results presented in this thesis.

Many thanks also go to Mr. Wade Lonsdale of B3 Electronics (and ECU PhD candidate) whose timely advice and experience with the voltammetric procedures associated with the PDV6000*plus* instrument and previous work with bismuth films were an important source of assistance.

I also expressly thank my reviewers, Dr. John Coumbaros and Mr. Peter McCafferty, for granting me some of their precious time to assess my proposal and also my thesis. Thank you as well, for access to samples and instruments at the Chemistry Centre, WA, especially Dr. Kari Pitts for her time with the optical microscope.

Additionally, I would like to thank the School of Natural Sciences Panel for their support in granting me the funds I required to complete my research.

Finally, thanks to the staff at ECU, for their help and good morale especially Mrs. Yvonne Garwood and Mrs. Lisa Skepper, who made my days a little lighter.

GLOSSARY OF TERMS

%RDS	percent residual standard deviation
Au	gold
Ba	barium
Bi	bismuth
BiE	solid bismuth electrode
BiFE	bismuth film electrode
Deposition Potential	the chosen potential with which the analyte is concentrated at the working electrode for a specified time
C-SWV	cyclic-square wave voltammetry
DP-ASV	differential pulse anodic stripping voltammetry
GCE	glassy carbon electrode
GSR	gunshot residue
Hg	mercury
HMDE	hanging mercury drop electrode
HNO_3	nitric acid
Hold Potential	the working electrode is held at the Hold potential for the specified time to allow equilibration of the working electrode prior to measurement
ICP-MS	inductively coupled plasma mass spectroscopy
KCl	potassium chloride
KI	potassium iodide
µg/L	micrograms per litre
mg/L	milligrams per litre
$LiClO_4$	lithium perchlorate
LOD	limit of detection
LS-ASV	linear sweep anodic stripping voltammetry
Measurement Start Potential	the point from which the instrument takes measurements until the designated Stop potential is reached
M	moles per litre
mM	millimoles per litre
Pb	lead
Sb	antimony
SW	square wave voltammetry
TMACl	tetramethylammonium chloride

LIST OF TABLES

Table 13. Differential Pulse potential delivery, GCE, 0.05 M KCl + Hg 5ppm electrolyte solution, 60 sec deposition time (t_{dep}), deposition potential (dp) = -2500 mV, Ba 50 ppb + Pb 50 ppb, altering the scan rate for investigation of peak height and optimal speed.

Table 14. Peak heights for change in deposition time at deposition potentials ranging from -3000V to -2400 mV, Ba 10 ppb, 0.05 M KCl, differential pulse, 100 mV/s.

Table 15. Barium concentrations found in 10 drinking water samples in Perth, WA using voltammetric analysis.

LIST OF FIGURES

Figure 11. Change in response for lead (10 ppb) at different deposition potentials and deposition (accumulation) times.

Figure 12. Solid electrode surfaces photographed using *Leica* microscope; [A] – solid bismuth electrode (BiE), [B] – solid gold electrode (Au), [C] – glassy carbon electrode (GCE), [D] – glassy carbon electrode with bismuth film, [E] – solid gold electrode with mercury film and [F] – glassy carbon electrode with mercury film.

Figure 13. Voltammograms of working electrodes in KCl electrolyte: [A] bare Au electrode (Ba 100 ppb), [B] bare BiE before conditioning and [C] bare Bi electrode (Ba 20 ppb) after two conditioning runs.

Figure 14. Voltammograms of GC working electrodes in KCl electrolyte: [A] pre-conditioning (Ba 10 ppb + Pb 10 ppb), [B] post-conditioning (Ba 10 ppb + Pb 10 ppb). The Ba peak is seen at -2058 mV and the Pb peak at -750 mV.

Figure 15. The surface of the glassy carbon electrode as seen through a microscope [A] after harsh polishing with fine grit sandpaper, and [B] re-polished correctly. The scratched surface of the electrode in A is clearly visible. The photographs in the middle are close-ups of the electrode surfaces shown on the left. Voltammograms depicting the electrode outputs associated with each are on the right.

Figure 16. Capacitance peaks for Ba 500 ppb and Pb 10 ppb on Au- *in-situ* Hg electrode system.

Figure 17. [A] Voltammogram showing Ba peak height of 2.58 μA at -2055 mV and Pb peak at -700 mV on the right, [B] linear range for Ba 20 – 100 ppb using Au-Hg film electrode ($r^2 = 0.988$).

Figure 18. Capacitance peaks for Ba (10 ppb) and Pb (1 ppb) on GCE-Hg film electrode system.

Figure 19. Capacitance peaks for Ba (200 ppb) and Pb (10 ppb) on GCE-Bi film electrode system.

Figure 20. Capacitance peaks after t_{dep} of 60 sec at dp = -2500 mV for Ba 100 ppb and Pb 100 ppb generated using bismuth electrode in [A] 0.02 M KCl and in [B] 0.1M TMACl.

Figure 21. Capacitance peaks produced after t_{dep} of 30 sec for Ba (50 ppb) and Pb (50 ppb) at -2500 mV, 100 mV/s on the GCE-*in-situ* Hg electrode system.

Figure 22. Mean peak heights for Ba obtained during voltammetric analyses with varying concentrations of mercury. The dotted line indicates the optimum concentration of Hg in-situ.

Figure 23. [A] Linear range from 10 - 160 ppb ($r^2 = 0.994$) for GC electrode using parameters of 0.02 M KCl + Hg 5ppm (0.0015 M HNO_3), t_{dep}= 30 sec, dp= -2400 mV, 100 mV/s. Ba 10 – 160 ppb. [B] Superimposed voltammograms from [A] showing increasing Ba concentrations.

Figure 24. [A] Linear range from 5 - 80 ppb ($r^2 = 0.997$) for GCE, 0.02 M KCl electrolyte + Hg 5ppm (0.0015 M HNO_3) + 63 µL 3% HNO_3, t_{dep} = 30 sec, dp =-2500 mV, 100 mV/s. [B] Superimposed voltammograms from *A* illustrating linear increase of peaks and [C] linear range from 5 - 40 ppb ($r^2 = 0.999$) for the same parameters as *A* but t_{dep} was increased to 60 sec.

Figure 25. Comparison of ASV results to ICP-MS results.

Figure 26. Standard addition voltammogram of barium response in Craigie bore water sample, using glassy carbon (GCE) electrode in 0.02 M KCl electrolyte, t_{dep}= 30 sec, dp = -2500 mV, 100 mV/s.

Figure 27. Standard addition voltammogram of barium response in brake pad dust sample, using glassy carbon (GCE) electrode in 0.02 M KCl electrolyte, t_{dep} = 30 sec, dp = -2500 mV, 100 mV/s.

Figure 28. Voltammogram showing simultaneous detection of barium and lead in a GSR sample using glassy carbon (GCE) electrode in 0.02 M KCl electrolyte, t_{dep}= 30 sec, dp = -2500 mV, 100 mV/s.

CONTENTS

CHAPTER 1 – INTRODUCTION AND SIGNIFICANCE

1.1 BACKGROUND

Barium is a heavy metal belonging to the alkaline earth group (II) in the Periodic Table. It exhibits high reactivity in air and water, and therefore occurs naturally in the form of inorganic compounds rather than as a pure metal. It is most commonly found as barite ($BaSO_4$) or witherite ($BaCO_3$) but is also detectable as soluble salts; barium chloride ($BaCl_2$), barium nitrate ($Ba(NO_3)_2$) and barium hydroxide ($Ba(OH)_2$) in almost all surface waters on Earth [*1*]. Due to its reactivity, typical uses of barium metal are as a "getter" to remove remaining gases from vacuum tubes and in the manufacture of other metals and alloys [*2*]. Myriad applications exist for barium compounds including the hydroxide used in greases, lubricating oils and plastics stabilizers, and the chloride used in water softening, dyeing, glass, and pigments in cosmetics and drugs [*3*]. Barium nitrate and the peroxide form are used in fireworks, detonators and tracer bullets; the carbonate is a rodenticide and provides lustre in glass, brick and clay products. The mined sulphate (barite) is applied as a weighting agent in drilling fluids for oil and gas wells and is also used in medicine as a radiopaque contrast medium in X-ray photography of the digestive tract [*3*].

With such widespread use of barium compounds in so many products, there is growing concern about the accumulation of barium compounds in the environment and their effects. Most barite mining occurs in the UK and USA and some environmental management concerns have been raised there about long-term accumulation of barium in river sediments and groundwater [*4*]. Although few studies exist in the literature, negative effects of dissolved barium on aquatic life in marine waters have been reported, specifically for bivalves and daphnids [*5, 6*]. Further, in a review by Kravchenko *et al.* [*6*], the authors note that recent expansion of shale gas drilling has increased the risk of barium pollution in groundwater and wells, igniting interest in scientific investigation of potential human and environmental health impacts since published information is limited.

1.1.1 ENVIRONMENTAL EXPOSURE

Soluble salts of barium are highly toxic to humans and ingestion or inhalation of the powders can be fatal [*3, 7*]. The slightly soluble carbonate is also toxic if swallowed due to digestion by stomach acid however acute poisoning cases are rare and mostly accidental through food preparation errors or deliberate suicides [*8, 9*]. Known adverse health effects related to human consumption of water highly contaminated with barium are cardiovascular disease, hypertension and muscle weakness [*10, 11*]. The main sources of drinking water contamination are usually from the erosion of natural deposits, discharge of drilling wastes and discharge from metal refineries [*6*]. In 2011 the World Health Organisation (WHO) revised its global drinking water guideline for barium from 2 mg/L down to 0.7 mg/L [*12*]. The US Environmental Protection Agency (EPA) [*7*] and Australian [*11*]

drinking water guidelines remain at 2 mg/L, despite studies reporting that chronic exposure to barium at low concentrations may be problematic [*6*]. As well, recent studies conducted in Bangladesh and Vietnam strongly suggest that the presence of barium promotes the carcinogenicity of arsenic in tube-wells [*13, 14*].

Monitoring human exposure to barium at industrial workplaces or through disposal of barium-rich industrial effluent is normally part of required heavy metals analyses in the interest of public health and environmental management. This is important because soluble barium compounds, such as the chloride, nitrate and hydroxide forms can be absorbed by the human body and are toxic to humans. The current data from animal studies on rats and mice show strong evidence that renal function is most adversely affected by long-term oral exposure to barium [*10, 11*].

1.1.2 SIGNIFICANCE

Routine analysis of heavy metals can be performed by a suite of analytical chemical methods; however, inductively coupled plasma mass spectrometry (ICP-MS) and flame atomic absorption spectrometry (FAAS) are the most commonly applied techniques because they are well established accredited methods [*7, 10, 11*]. Laboratory analyses using these methods are expensive, can be time-consuming and are not suitable for in-field analysis. An in-situ and inexpensive portable analytical method is an attractive alternative in remote locations or when immediate and on-site results are a necessity. Voltammetry could provide such an alternative technique. Voltammeters are easily available, portable and relatively cheap compared with ICP-MS and FAAS, and anodic stripping voltammetry is one of several officially recognized techniques for the detection and speciation of metal ions in natural waters outlined in the National Water Quality Management Strategy [*11*].

1.2 ANODIC STRIPPING VOLTAMMETRY THEORY

Anodic stripping voltammetry (ASV) is an electro-analytical technique enabling detection of metals in various matrices [*15*]. ASV is relatively inexpensive and allows for the simultaneous determination of several metals. It exhibits high sensitivity for most metals and does not require any pre-concentration of the samples prior to analysis because the reduction step itself concentrates the metal ions. The limit of detection is ICP-MS comparable due to advances in electronics enabling measurement of micro currents [*16*].

The ASV technique consists of three steps performed using an electrochemical cell fitted with three electrodes: the working, reference and counter electrodes [*17*] as shown in Figure 1. The counter electrode is used to avoid the potential drop due to solution resistance in a 2-electrode system.

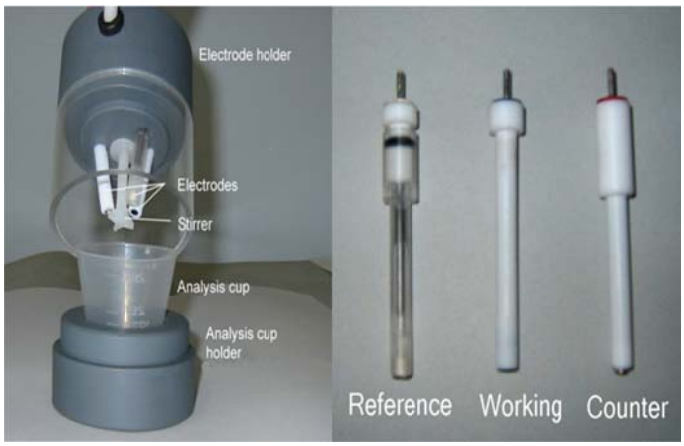

A B

Figure 1. [A] The 3-electrode cell, illustrating working, reference and counter electrodes held in the top compartment around a plastic stirring bar in the centre. [B] The electrodes shown are (from left to right) Ag/AgCl, glassy carbon and coiled platinum (Source: Dr. M. Wajrak).

A removable analysis cup sits in the bottom compartment and acts as the reaction vessel for electrolyte and sample. The potential applied to the working electrode is precisely controlled relative to the reference electrode while the current to be measured passes between the working electrode and the counter electrode [*27*]. Firstly, a cathodic or anodic potential is applied to the working electrode whilst stirring the solution (Figure 2A). The metal ions reduce and electroplate onto the electrode, concentrating them; $M^{n+}_{(aq)} + ne^- \Rightarrow M_{(s)}$ (Figure 2B). Next, stirring is stopped, and then the applied potential is reversed, stripping the deposited metals off the electrode (oxidation), which generates a current that can be measured; $M_{(s)} \Rightarrow M^{n+} + ne^-_{(aq)}$ (Figure 2C). Each metal generates a characteristic current and can be measured by quantification of both peak magnitude and the area beneath the curve (Figure 3).

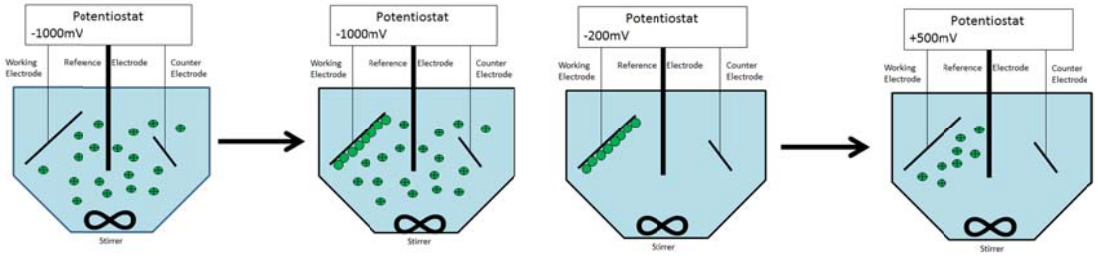

A B C

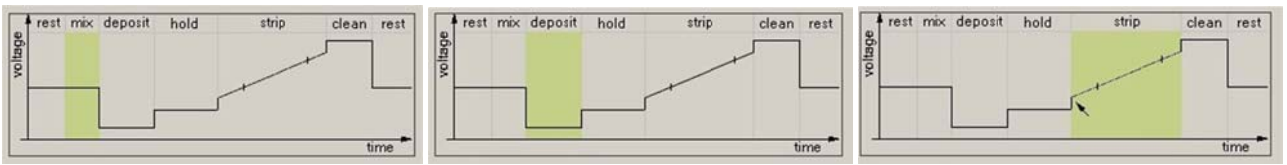

Figure 2. Illustrating the 3 steps in ASV: [A] stirring, [B] reduction and hold (deposition at negative potential), [C] stripping at progressively more positive potential, (Source: Mr. P. Lewtas, MSc. Thesis, ECU, 2014).

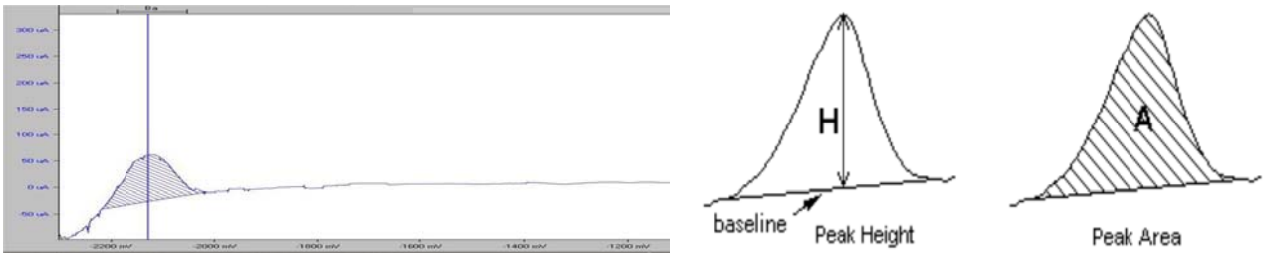

Figure 3. A typical voltammogram for Ba showing the stripping potential (-2100 mV) at which a current (85 µA) is generated. Peak height and area are both directly proportional to Ba concentration (Source: Dr. M. Wajrak).

The potential waveform employed at the stripping step can be linear, differential pulse or square wave, the choice of which is very reliant on the type of electrode, analyte and electrolyte to be employed in the analysis (Figure 4). Linear sweep is the simplest but can also be the least sensitive so differential pulse is sometimes preferred for the net current value taken from two points.

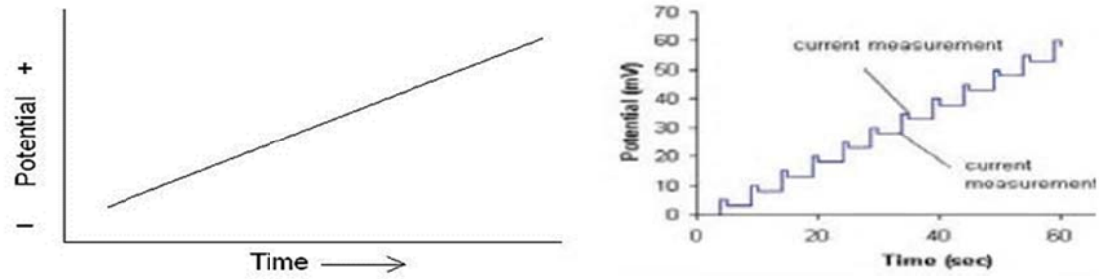

A B

Figure 4. Depicted on the left and right respectively, are the [A] Linear Sweep, and [B] Differential Pulse types of waveforms generated by the potentiostat during voltammetric analysis (Source: Dr. M. Wajrak).

1.2.1 DETECTION OF BARIUM USING VOLTAMMETRY

Sensitive methods have been developed for a wide array of metals including Pb, Cu, Cd and Zn. Indeed, voltammetry is the technique of choice for in-situ and in-field monitoring of certain trace metals; unfortunately, barium (Ba) still remains a challenge [*15, 18, 19*]. Electrochemists have reported difficulty in reliably quantifying Ba with ASV, because of the very high negative deposition potential of -2.92 V in both acidic and alkaline conditions [*20*]. This causes evolution of gases (i.e. H_2, Cl_2), via the oxidation and reduction processes occurring during electrolysis, which build up at the working electrode and interfere with the Ba signal [*18*]. Amalgams formed between H_2/Hg can also distort the Ba peak and interfere with the analytical signal [*21*]. Au and Hg films

used to coat electrodes tend to deteriorate quickly at very negative potentials making reproducibility difficult [*16*]. Dissolved oxygen can cause hysteresis in the voltammogram between the sample and the blank, due to the generation of background noise in ASV. This appears as a shift in the peak and therefore deoxygenation of the sample is often required [*22*].

Woolever and Dewald [*18, 22*] were the first to detect Ba using ASV simultaneously with Pb in gunshot residue (GSR) using mercury (Hg) film on glassy carbon electrode. Various electrolytes were investigated with the aim to alter the deposition potential to a less negative value, but they ultimately selected dp = -2400 mV, while the peak potential for Ba changed depending on the electrolyte. Standard deviations were large due to H_2 evolution however, and Ba detection failed for low concentration samples. Other researchers [*19, 21*] also attempted barium analysis by ASV using a mercury-film working electrode with various electrolytes, such as $LiClO_4$, KCl and KI, and they all reported issues with reproducibility and interferences from gases. The reported deposition times were 1 – 6 minutes; hence gas evolution was inevitable at such negative potentials (Table 1).

As can been seen in Table 1, GCE with mercury film is the most commonly studied electrode, however, there are now other electrodes available, such as bismuth (Bi) electrode, which maybe a possible alternative to GCE/Hg system. Thus, although achieving a robust method for the determination of barium by ASV is difficult predominantly because of its very negative standard reduction potential, a thorough systematic study of the GCE/Hg system has not been completed and other alternative electrode systems have not been investigated [*19*].

Table 1. Summary of experimental conditions previously employed in the detection of barium by voltammetry in the literature reviewed. LS = linear sweep; DP = differential pulse; C-SWV= cyclic-square wave voltammetry.

Year	Reference	Working Electrode	Technique	Electrolyte	Deoxygenation	DepositionTime
2000	Woolever et al. [*18*]	GCE + Hg film	DP-ASV	0.1 M $LiClO_4$	N_2	6 min
2001	Kovaleva et al. [*25*]	Ag + Hg film	LS-ASV	0.1 M KCl	Ar	3 min
2001	Woolever et al. [*27*]	GCE + Hg film	DP-ASV	0.1 M TEABr	N_2	3 min
2005	Agrawal et al. [*28*]	GCFE	DP-ASV	0.1 M TMACl	N_2	2 min
2009	Wajrak [*23*]	GCE + Hg film	LS-ASV	0.5 M KCl	No	1 min
2012	Vuki et al. [*30*]	GCE + Hg *in-situ*	C-SWV	0.1 M $LiClO_4$	No	3 min

1.2.2 THE EFFECT OF ELECTRODE AND ELECTROLYTE

In ASV, the type of electrode is important in detecting different chemical species because chemical reactions are involved between the metal ions in solution, the electrolyte and electrode surface [*24*]. No electrode is ideal for all situations. Species fall into one of five categories classified by Anson [*33*], and tend to adsorb on the electrode surface to different degrees depending on their affinity for the substrate and forming ionic or covalent bonds. Both Ba^{2+} and Hg^{2+} are Class III cations that are inductively adsorbed via Class IB anions such as Cl^-. Without the anionic bridge formed by the Cl^- ions, the cations cannot adsorb to the surface of the electrode [*33*].

Adsorbates can block or enhance the electrode response to an analyte under investigation. Adsorption is considered an equilibrium process between the solvent/electrolyte (S), analyte or adsorbate (A) and the electrode (E) as illustrated in Figure 5. Surface roughness of the electrode affects performance of solid electrodes because cleanliness, uniformity and oxidation of the surface layer all affect the electron transfer process either negatively or positively [*24*], which affects the height, width and shape of the capacitance peak produced for the analyte of interest during the oxidation/stripping step.

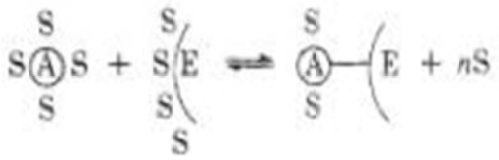

Figure 5. Adsorption at an electrode as an equilibrium process where S is the solvent/electrolyte, A is the adsorbate and E is the electrode. To form a bond to the electrode, the adsorbate will lose some of its solvating molecules and displace the solvent molecules adsorbed on the electrode [*33*].

The solid electrodes investigated here, were glassy carbon, solid gold and solid bismuth. Glassy carbon was modified with both mercury and bismuth films, whereas gold was modified with mercury only and bismuth remained bare metal. Advantages to glassy carbon (also known as vitreous carbon) are its modest cost, slow oxidation kinetics, impermeability to liquids and gases, high hydrogen overvoltage and wide potential range [*24*]. Polishing procedures for glassy carbon can be tedious and variable between types of applications but its performance tends to be excellent with regard to reproducibility and background stability.

Solid gold electrodes can be used over a wide pH range and have a good cathodic potential window, but drawbacks are low hydrogen overvoltage, high cost and requires frequent polishing [*16*].

Mercury film on carbon and gold electrodes are advantageous in ASV as mercury forms amalgams with many metals, producing peaks with excellent resolution. Films provide a replaceable and reproducible surface too and one advantage of gold-mercury film electrode over carbon-mercury film is that it can withstand very negative potentials without damage [*P. Lewtas, personal communication, 7th September 2015*].

In 2005, Wang reviewed bismuth electrodes as a 'green' alternative to Hg electrodes and commented that bismuth electrodes need to be more thoroughly studied [*26*]. Bismuth electrodes have a wide cathodic potential window and are less susceptible to background interference from oxygen; two attractive features for possible Ba analysis. In addition the two metals (Ba and Bi) have been recently used together in some newer alloys [*26*], indicating potential affinity between the two metals, which is important for voltammetry.

Solid bismuth electrodes (or bulk bismuth disks) are very similar to bismuth films apart from exhibiting slightly lower hydrogen overvoltages and have been developed as a non-toxic alternative to mercury electrodes [*26*]. Bismuth performs well in ASV for heavy metals with standard reduction potential more negative than bismuth (-300 mV), offering high hydrogen overvoltage, low susceptibility to oxygen interference, a wide cathodic window and good peak resolution.

Although solid electrodes are an attractive choice over films deposited on electrodes, which tend to deteriorate with analytical runs, solid electrodes require polishing and chemical conditioning before detection of a particular analyte [*24*]. Polishing physically creates a smoother, more even surface for uniform distribution of the accumulating analyte, producing a better signal. Chemical conditioning activates the electrode towards the analyte of interest and may take a number of voltammetric runs until a capacitance peak is seen for the analyte and/or the peak stabilises at a certain height for a known concentration of analyte [*16*].

In ASV, the sensitivity of the electrode is usually a strong function of deposition potential [*24*] so altering that value and the amount of time allowed for deposition (t_{dep}) can increase or decrease the accumulation of analyte at the electrode, thereby altering the current generated at the stripping potential for that analyte [*15*]. In the case of barium, it is beneficial to use a less negative deposition potential for the shortest t_{dep} to prevent signal interference from hydrolysis of the electrolyte itself [*19, 21*]. The optimal deposition potential is an adjustment between some loss of accumulation and better resolution of the stripping peak.

The choice of electrolyte also has a major influence on the deposition potential, selectivity of the electrode to the analyte and the potential area where the capacitance peak of the analyte is produced and seen on the voltammogram [*24*]. The electrolyte also enhances or suppresses chemical reactions in solution and production of compounds that produce signal interference [*22*]. Choice of

electrolyte therefore, is important in altering peak position to avoid overlap with other analyte peaks, thereby reducing interferences.

Another consideration for electrolyte choice was its ability to endure scanning to very negative potentials with limited effects from electrolysis [*24*]. Tetraalkylammonium halides, $LiClO_4$ and KCl electrolytes can resist electrolytic breakdown until approximately -2900 mV, thus are the electrolytes of choice in voltammetric detection of barium. For this project, the intention was to use the least toxic electrolyte possible and to pair it with the 'greenest' electrode without compromising sensitivity to barium, so KCl was most extensively investigated.

Electrolyte concentration is important for conductivity and quantity of supporting ions in the solution [*24, 34*]. Having a high quantity of ions ensures that the voltage drop that occurs between the electrode and the bulk solution happens within a distance of 10-20 Å, and the electron transfer reactions occur at the traditionally accepted rate constants. The typical value for electrolyte concentration is 0.1 M or higher and this is consistent with the literature (Table 1).

The type of potential delivery influences the sensitivity of the instrument in measuring the current. Linear sweep is least sensitive but is fast and simple and has been used for the voltammetric detection of barium (Table 1). The majority of researchers have preferred differential pulse because being able to subtract the background current from the Faradaic current produces a net current that is both more accurate and sensitive [*24, 36*]. Scan rate, also known as sweep rate, is the rate at which the potential is applied and affects the speed of stripping [*34*]. The amount of electrons released is the same but over a shorter or longer time frame, and depending on the kinetics of the chemical reactions in the solution undergoing analysis, can affect peak heights obtained from analytes [*35*].

1.3 PROJECT RATIONALE AND AIMS

1.3.1 RATIONALE

A gap in the literature exists pertaining to barium analysis by ASV. This project, therefore, is predominantly focused on the fundamental development of an ASV method for the detection of barium. The pervasive use of barium compounds in our society and the toxicity of the soluble compounds, such as barium nitrate, which is a component of gunshot residue, prompt the monitoring of barium in the environment in order to reduce human exposure. Accordingly, reliable, onsite detection of barium would be desirable. The secondary focus of this project therefore, was the application of the ASV method to analysis of barium in several types of samples, such as

drinking water, GSR and brake pad dust as an alternative to current laboratory-based methods, such as ICP-MS and FAAS.

A rapid barium detection method could be an advantage for environmental consultants, because it would allow for monitoring of water supplies in the vicinity of oil and gas fracking activities [*6*]. Trace metal detection of barium can also be used as an indicator of vehicle brake pad deterioration [*25*]. Brake dust has recently been shown to be a major contributor of particulate matter in urban air pollution following studies conducted in the UK [*42*]. Barite is a filler material in brake pads and has been defined as a unique tracer to separate brake wear pollution from the wear of other car parts.

Additionally, the ability to detect barium in-field is potentially a useful tool for screening gunshot residue samples (GSR) collected by forensic personnel at sites of interest. O'Mahony & Wang [*19*] point out that the presence of barium is a stronger indicator of GSR compared with lead as there are fewer environmental sources that could account for its presence. Pre-screening of samples could eliminate the number of negative samples sent for scanning electron microscopy with energy dispersive X-ray analysis (SEM-EDX), and deliver a considerable cost-savings benefit to forensic police departments.

1.3.2 PROJECT AIMS

The two major aims of this project are:

1. To develop and validate a cost-effective, reliable and robust, in-field ASV method for quantitative determination of barium using a PDV6000*plus* instrument.

2. To apply the optimized voltammetric method for the quantification of barium in various samples, including water samples, industrial effluent and GSR samples and compare to ICP-MS results.

CHAPTER 2 – EXPERIMENTAL

2.1 EXPERIMENTAL DESIGN

Development of a voltammetric method for the determination of barium was undertaken and the method applied to quantitative analyses of various samples possibly containing barium. Systematic trialing of various electrodes and electrolytes in controlled voltammetric tests on known quantities of barium standards achieved the optimum method of detection. The optimized ASV method for barium detection was then applied to various samples and metal concentration was determined using standard addition method with correlation coefficient (R^2) being greater or equal to 0.99 and the results compared to ICP-MS.

2.2 CHEMICALS

All metal standards purchased were ICP grade from Australian Chemical Reagents (ACR). 1000 mg/L metal standards in 2% nitric acid solution were obtained from ACR for mercury, lead, barium, antimony and bismuth. Analytical grade potassium chloride ≥99.9995% (Fluka), sodium chloride ≥99.999% (Fluka), sodium acetate ≥99.999% (Fluka), tetramethylammmonium chloride ≥97% (USA) and acetic acid ≥99.5% were purchased from Sigma-Aldrich (Sydney, Australia). Nitric acid 69% Suprapur® was purchased from Merck (Australia). All solutions were prepared with deionized water generated by a Millipore Milli-Q water system (Bedford Massachussetts, USA) with resistivity not less than 18.2 $M\Omega.cm^{-1}$ at 25°C. Certified GhostWipes™ Standards of 100 µg barium per wipe were purchased from EnviroExpress.

2.3 SOLUTIONS

2.3.1 STANDARDS

Separate 20 ppm working standard solutions of barium and lead were prepared daily in voltammetric analysis cups, diluting 400 µL of the primary standard in 19.6 mL Milli-Q water. Each analysis cup was covered with a watchglass to prevent evaporation loss and dust contamination. Certified GhostWipes™ Standards were prepared in 50 mL sample tubes and submerged in 15.0 mL 3% nitric acid solution to extract the metals. The extraction process was conducted by agitating sample tubes for 4 hours and allowing solutions to equilibrate for 24 hours.

2.3.2 ELECTROLYTES

100 mL of 2.0 M KCl stock solution was prepared with 14.91 g of potassium chloride accurately weighed on a Mettler AE200 analytical balance and dissolved in Milli-Q water. Working solutions ranging from 0.001–0.5 M were prepared from the stock solution, directly into 20 mL voltammetric analysis cups as required, with the addition of 100 µL of 1000 mg/L Hg standard to produce a mercury concentration of 5ppm. A 3% HNO_3 stock solution was prepared by diluting 15 mL

concentrated nitric acid in 485 mL of Milli-Q water. 1.0 M tetramethylammonium chloride (TMACl) stock solution was prepared using 10.96 g TMACl accurately weighed into a beaker on the analytical balance. The crystals were dissolved in Milli-Q water and the solution quantitatively transferred to a 100 mL volumetric flask and made up to the mark with Milli-Q water. Working solutions of 0.01 M, 0.1 M and 0.5 M TMACl were prepared in 20 mL voltammetric analysis cups from the stock solution as required. Acetate buffer (ClAc) solution was prepared by combining 7.3 g sodium chloride, 1.35 g sodium acetate and 0.6 mL acetic acid in a 500 mL volumetric flask and diluting appropriately with Milli-Q water.

A Eutech cyberscan pH/conductivity/TDS/^{o}C/^{o}F meter was used to measure pH and calibration was performed using Merck brand pH 4 and pH 7 buffers. Laboratory glassware was acid washed and thoroughly rinsed with Milli-Q water prior to use and supplied by Edith Cowan University.

2.3.3 FILMS

The use of thin and thick Hg films was required on carbon and gold electrodes respectively. A 5 ppm mercury plating solution was prepared with 100 µL of 1000 mg/L Hg standard in 19.9 mL ClAc for use with the glassy carbon electrode. For the gold electrode, a 500 ppm mercury plating solution was prepared with 10 mL of 1000 mg/L Hg standard in 10 mL ClAc. The 20 ppm bismuth plating solution was prepared using 400 µL 1000 mg/L Bi standard in 19.6 mL 0.1 M HNO_3 for use with the carbon electrode.

2.4 SAMPLE PREPARATION

All samples were prepared according to their type, altering the volume of electrolyte or sample solution dispensed into the analysis cup depending on the pH of solution or concentration of barium in the sample solution. Voltammetric runs for sample analysis were performed in the following order: a blank sample run at 0 sec t_{dep}, a sample analysis at 30 sec $t_{dep,}$ and up to four 10 µL standard additions of Ba (10 ppb) each for 30 sec t_{dep}. If a Ba peak did not appear at 30 sec t_{dep}, then the sample was run with 60 sec t_{dep}, or 120 sec or 240 sec t_{dep}, after which if no Ba peak had appeared on the voltammogram it would be considered to be below the limit of detection.

2.4.1 DRINKING WATER SAMPLES

Various types of Western Australian drinking water samples were collected: tap water, bore water, bottled water, and a sample from a rainwater tank. Samples were collected in 1L plastic bottles that were triple rinsed prior to filling. Bore water samples were collected by the property owners in Muchea, Bullsbrook, Craigie and Wangara, WA. Bottled water was purchased at a local supermarket and remained sealed until analysis. Tap water was collected from the author's home

kitchen faucet in Wanneroo, a drinking water fountain on the Joondalup campus at Edith Cowan University, and from a church in Bullsbrook where the patrons freely drink the supplied 'holy water', obtained from a faucet on the grounds.

Samples were diluted prior to voltammetric analyses. Samples were run as 2.0 mL aliquots, in 18.0 mL 0.02 M KCl electrolyte with a 100 µL aliquot of 1000 mg/L Hg standard in the 20 mL analysis cup. These quantities provided the electrolyte conditions of 0.02 M KCl and 5ppm Hg in the optimized method and not more than 1.5 mM HNO_3 content.

For ICP-MS analysis, a 9 mL aliquot of sample plus 1 mL 3% nitric acid were transferred to 15 mL sample tubes and sealed.

2.4.2 BRAKE PAD DUST SAMPLES

Vehicle wheel rims, brake calipers and brake pads were wiped with cotton cleaning patches or Ghostwipes™ in accordance with NIOSH (2009) procedures and placed in 50 mL sample tubes. Brake pads covered in loose dust were shaken into 50 mL sample tubes for dust particle collection. All samples were submerged in 15.0 mL 3% HNO_3 solution to undergo extraction for 24 hours and sent for ICP-MS analysis. For voltammetric analysis, up to 63 µL aliquot of sample was added to 19.37 mL of 0.02 M KCl + Hg 5ppm electrolyte solution, equal to 3.0 mM total content of HNO_3.

2.4.3 GUNSHOT RESIDUE SAMPLES

Ghostwipes™ containing GSR samples from a previous study were re-analysed using the optimized barium method. Surface samples were originally taken at a gun range in Swanbourne, Western Australia. 100 cm^2 sized surface areas were wiped using Ghost Wipe™ lead sampling wipes and placed into sealed sterile tubes. Gloves were worn to prevent contamination. Ghost Wipes™' were placed inside clean 15.0 mL sample tubes with 15.0 mL of 2% nitric acid added to each sample. Two controls were prepared by transferring 15.0 mL 2% nitric acid only to a clean sample tube and by placing an unused Ghost Wipe™ in another sample tube with 15.0 mL 2% nitric acid. All samples were agitated for approximately 4 hours at 500 mot/min, to speed up the extraction process. After agitation, all samples were allowed to equilibrate for 24 hours. Samples were analysed using ICP-MS and ASV. For voltammetric analysis, a 63 µL aliquot of sample was transferred to 19.37 mL of prepared electrolyte in a voltammetric analysis cup in preparation for analysis by ASV. Total volume of sample and electrolyte contained a total concentration of 3.0 mM HNO_3.

2.4.4 ENVIRONMENTAL SAMPLES

Thirteen prepared water samples were received from ChemCentre, acidified to < pH 2 with nitric acid in 50 mL plastic sample containers. Samples had been previously analysed by ICP-MS and were collected from bores at locations in the Pilbara. A 63 µL aliquot of sample was transferred to 19.37 mL of prepared electrolyte in a voltammetric analysis cup in preparation for analysis by ASV.

Total volume of sample and electrolyte contained a total concentration of 3.0mM HNO_3, as per the optimized method.

2.5 INSTRUMENTATION

2.5.1 ANODIC STRIPPING VOLTAMMETRY

All measurements were conducted on a Modern Water PDV6000*plus* instrument (portable, digital voltammeter) equipped with a 3-electrode cell and plastic analysis cup, displayed previously in Figure 1. The working electrodes were manufactured at B3 Electronics, Osborne Park Western Australia. These electrodes were glassy carbon, solid gold and solid bismuth, and each electrode had a surface area of 3 mm^2. The reference electrode was Ag/AgCl/1.0 M KCl and the counter electrode was a platinum wire coil. An IBM Thinkpad laptop (Model number 23736YM) was used in connection with the PDV6000*plus* potentiostat and controlled via Voltammetric Analysis Software (VAS) version 5.1 to generate the voltammograms (Figure 6).

Figure 6. PDV6000plus portable voltammetric analysis instrument set up in conjunction with a laptop computer. An electrochemical cell is shown at bottom left corner.

2.5.2 ELECTRODE PREPARATION

The 5 ppm mercury plating solution was run at -1000 mV for 300 sec on the carbon electrode for a thin film [*19*], and the 500 ppm solution run for 600 sec to form a thick film as required for the gold electrode [*41*]. The 20 ppm bismuth plating solution was run at -1100 mV for 300 sec on a carbon electrode [*36*]. Electrodes were polished for approximately 60 sec with Milli-Q water on a Buehler polishing pad and inspected under a microscope prior to the plating procedure and also prior to use without film modification.

2.5.3 INDUCTIVELY COUPLED PLASMA – MASS SPECTROMETRY / ATOMIC EMISSION SPECTROSCOPY

Laboratory technicians at ChemCentre, WA, performed the ICP-MS analysis of all samples except the environmental samples, which were analysed with ICP-AES. The metals Ba, Pb and antimony (Sb) were analysed by ICP-MS method iMET1WCMS (APHA 3125) and calcium (Ca) was analysed by ICP-AES method iMET1WCICP (APHA 3120). For the environmental samples, ICP-AES methods iMET1WTICP (unfiltered) and iMET1WCICP (filtered) were used for analysis of Ba. Lines used were Ba 455.403 nm, Ba 233.527 nm and confirmation line Ba 493.408 nm.

2.6 STATISTICAL ANALYSIS

All method development results were expressed as mean values and calculated using Excel for Mac 2011, Version 14.0.0. Sample results were calculated using VAS 5.1 linear regression analysis. Comparative analysis between ASV and ICP-MS was performed using IBM SPSS Statistics.

CHAPTER 3 – RESULTS AND DISCUSSION

3.1 OVERVIEW

In the development of an ASV method for barium detection, one of the key factors is the choice of electrode. A review of the literature concerning voltammetric detection of barium (key papers summarized in Table 1, Section 1.2.1) indicated that glassy carbon was the most commonly employed electrode in combination with linear sweep or differential pulse mode for potential delivery. Consequently, the glassy carbon electrode system was used as a starting point for the determination of key voltammetric parameters, which are crucial for the successful detection of the analyte of interest.

However, because the literature showed mixed results with the glassy carbon electrode, other electrodes were also investigated, in particular gold, following the work by Saläun [*16*], and bismuth, following the work by Wang [*26*], keeping in mind that in order to develop an in-field voltammetric method for barium, avoiding deoxygenation of the electrolyte/sample solution was an important factor for portability [*26*].

Therefore, the method development involved firstly, defining the initial voltammetric parameters using the glassy carbon electrode (Section 3.2), secondly, investigating different types of electrodes with various electrolytes (Section 3.3), and thirdly, once the most promising system was established and investigated more thoroughly (Section 3.4), validating the method by determining linear working range, limit of detection and stability along with some examination of interferences (Section 3.5).

Following optimisation, the method was then applied to a variety of samples and those results were compared to analysis of those samples by ICP-MS and/or ICP-AES (Sections 3.6 and 3.7).

Pb detection was also investigated in conjunction with Ba because of possible application of the method to GSR samples; therefore some results for Pb are included in the discussion.

3.2 VOLTAMMETRIC PARAMETERS

Initial parameters were chosen based on the standard reduction potential of barium, which has been determined to be -2.92V at standard temperature and pressure [*20*], and linear sweep was the type of potential delivery first used. As shown in Figure 7, a -3000 mV deposition potential was used with the intention of decreasing it as much as possible during the optimisation process.

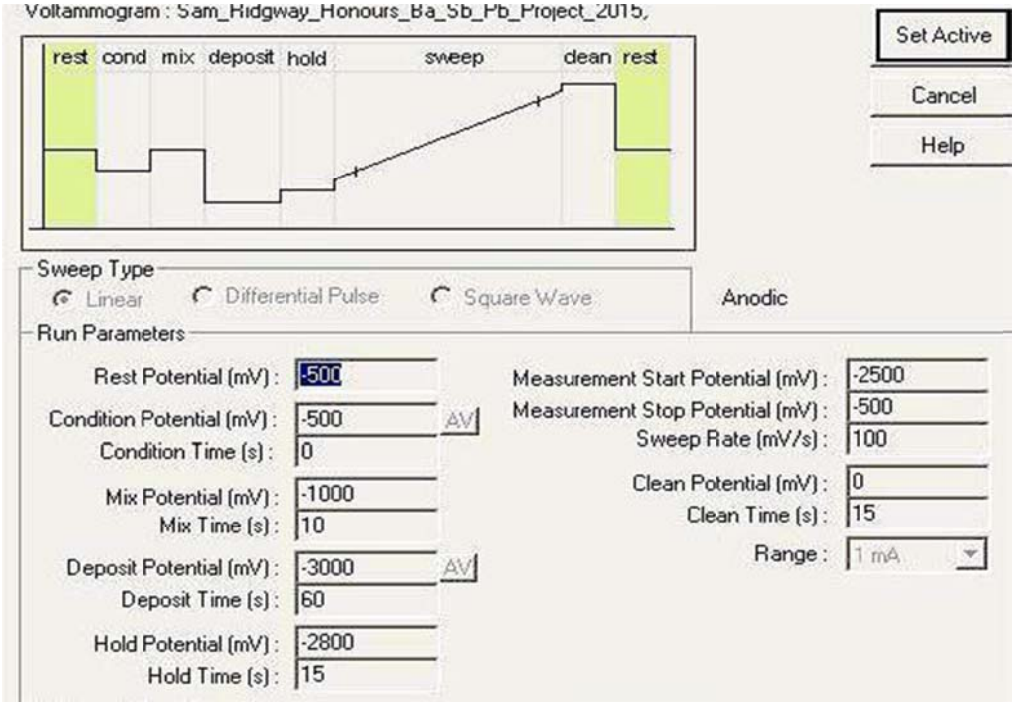

Figure 7. The key voltammetric parameters determined for the first analysis of Ba on a carbon electrode with mercury film.

The Rest Potential was set at -500 mV and is the voltage set at the working electrode when the instrument is at rest. The working electrode is held at the Condition potential and Mix potential for the assigned times prior to deposition, to condition the electrode towards the analyte(s). Analyte(s) are concentrated on the working electrode at the deposition potential during the Deposit time (t_{dep}). Sixty seconds was chosen for t_{dep} initially, but again with the objective of decreasing that time to reduce production of gases. The working electrode is kept at the Hold potential for a certain time to enable equilibration of the working electrode prior to measurement.

Measurements are performed between the Measurement Start and Stop potentials, therefore, based on the literature [*18, 22, 30*], Start/Stop potentials of -2500 mV to -500 mV were set to capture the Ba peak expected to appear at approximately -2000 mV. The Sweep Rate (or scan rate) determines the speed at which measurements are executed so a rate of 100 mV/s was specified based on sweep parameters used in previous work [*23*]. The working electrode is cleaned (stripped) at the Clean potential for a designated time, and for this project, was set for 15 sec at 0 mV so as not to strip the Hg film. The Range is the maximum current that will be measured by the instrument and can be limited to 10 µA or extended to 3 mA depending on expectations (Figure 7).

3.2.1 SWEEP POTENTIAL DELIVERY

Initially, linear sweep delivery was used in 0.5 M KCl electrolyte with Hg 1ppm – Hg 100 ppm with high quantities of Ba (100 ppb – 5 ppm), in order to find the Ba stripping region and confirm the Ba peak. The initial resultant peaks were either non-existent, very strangely shaped or poorly resolved (data not shown). The baseline was very noisy or steeply sloped, or both and peaks were not reproducible over a number of runs. A Ba peak of 15.29 μA was detected using linear sweep (0.05 M KCl + Hg 5 ppm, 500 mV/s, at deposition potential of -3000 mV), for 50 ppb concentration of Ba (Table 2). A Ba peak did not appear using linear sweep at the less negative dp = -2500 mV.

When detection was attempted with differential pulse potential delivery (0.05 M KCl + Hg 5 ppm, 100 mV/s, dp = -3000 mV and -2500 mV), Ba peaks of 36.93 μA and 87.27 μA were produced for Ba concentrations of 50 ppb at -3000 mV and -2500 mV respectively. As well, at dp = -3000 mV both techniques required a deposition time (t_{dep}) of 60 sec, whereas at dp = -2500 mV only t_{dep} of 30 sec was required to detect peaks.

Table 2. Capacitance peak heights for Ba using linear sweep (LS-ASV) and differential pulse (DP-ASV) potential delivery techniques.

Sweep type	Deposition potential (mV)	Deposition time (s)	Ba concentration (ppb)	Peak height (μA)
LS-ASV	-3000	60	50	15.29
LS-ASV	-2500	30	50	-
DP-ASV	-3000	60	50	36.93
DP-ASV	-2500	30	50	87.27

These results clearly demonstrated the superior sensitivity of differential pulse potential delivery for the detection of barium, particularly at less negative deposition potential and so DP-ASV technique was selected for the duration of the project.

3.2.2 SWEEP RATE

Using linear sweep, the Ba peak was seen consistently between -2180 mV to -2080 mV and the Pb peak at -880 mV to -710 mV. With linear sweep however, the baseline noise was indistinguishable from the Ba peak for 50 and 100 mV/s sweep rates (Figure 8). The optimum rate was 500 mV/s using linear sweep technique due to the non-linear behavior of Ba and resolution of peaks on the voltammograms. Peak heights for Ba and Pb at 500 mV/s were 15.26 μA and 16.6 μA respectively. Wu reported similar results for Pb and Cu [*35*] using fast sweep rates with linear sweep, concluding that slower reaction kinetics of Cu was the reason for its non-linear behavior and is possibly the case here with barium.

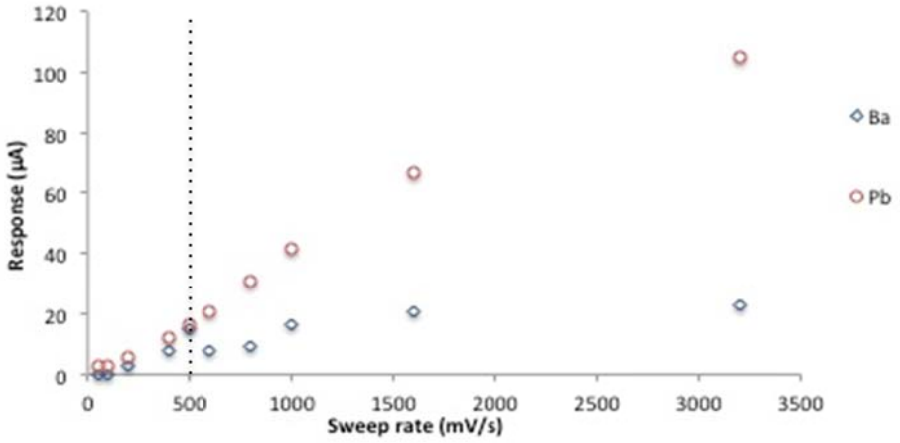

Figure 8. Investigation of sweep rate for linear sweep potential delivery. The dotted line delineates 500 mV/s as the optimum rate for Ba and Pb, chosen because the response for Ba after 500 mV/s is not linear compared with Pb.

Stripping regions for both analytes shifted slightly when using differential pulse. The Ba peak appeared between -2260 mV to -2000 mV and the Pb peak at -860 mV to -580 mV. Ba was not seen at 200 and 300 mV/s sweep rates due to an extremely noisy baseline at those rates (Figure 9). In general however, the baseline and resolution of peaks was better using differential pulse technique.

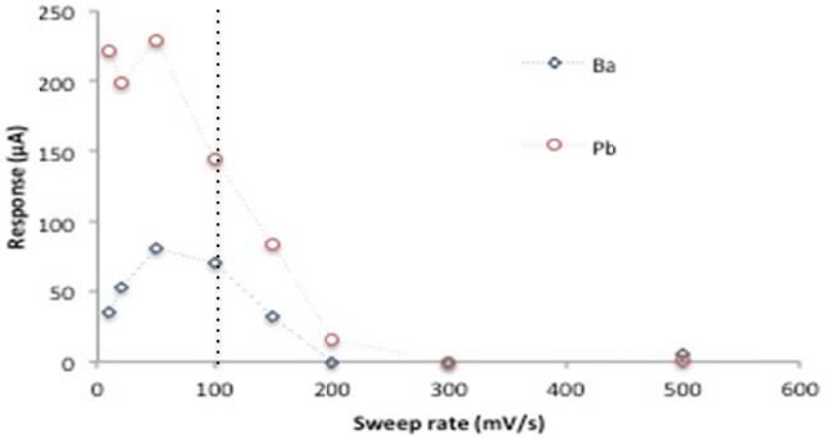

Figure 9. Investigation of sweep rate for differential pulse delivery. The dotted line indicates the optimum rate for Ba and Pb. Note: Although 50 mV/s produced higher peaks, they were poorly resolved compared with peaks generated at 100 mV/s due to higher noise in the baseline.

Although values for peak heights were larger using a 50 mV/s sweep rate, better peak resolution and smoother baseline found at 100 mV/s favoured the latter as the optimum choice. All peak height data obtained for the sweep rate for LS-ASV and DP-ASV is tabled in the Appendix.

3.2.3 STEP DURATION AND PULSE HEIGHT

Step duration and pulse height are parameters reported for the method when using DP-ASV and can be modified; however, these were not optimised during this project due to time constraints. Standard values based on extensive previous research and recommended by the manufacturer of the instrument were taken for both parameters. Consequently, the optimal pulse height was 50 mV and step duration was 10 ms when using differential pulse at a scan rate of 100 mV/s.

3.2.4 DEPOSITION POTENTIAL

Deposition potential (dp) was initially investigated with 0.05 M KCl using differential pulse at 100 mV/s from dp = -3000 mV to dp = -2300 mV with Ba and Pb standards. Deposition times were 10, 30, 60 and 120 sec for each potential (Figures 10 & 11). Both Ba and Pb standard concentrations were 10 ppb. A 30 sec, 0.05 M KCl / 5 ppm Hg blank for each deposition potential (dp) was used. The optimum dp for Ba was clearly -2500 or -2400 mV, and when each was tested, dp = -2500 mV showed better stability and reproducibility over multiple runs compared to dp = -2400 mV.

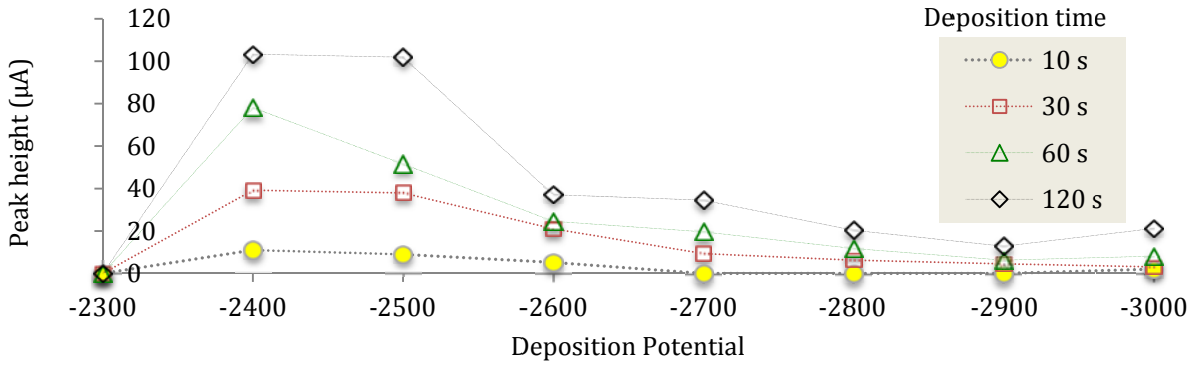

Figure 10. Change in response for Ba (10 ppb) at different deposition potentials and deposition (accumulation) times.

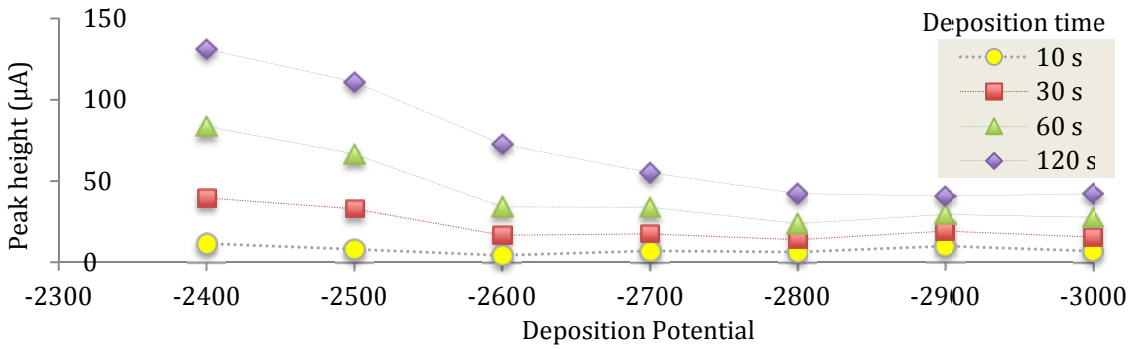

Figure 11. Change in response for Pb (10 ppb) at different deposition potentials and deposition (accumulation) times.

In summary, the voltammetric parameters to be used and then optimized for each electrode system tested are: differential pulse potential delivery using a sweep rate of 100 mV/s with pulse height of 50 mV and 10 ms step duration, and a deposition potential of -2500 mV for 30 sec minimum deposition time.

3.3 INVESTIGATION OF ELECTRODE TYPE

As previously stated in Chapter 1, Section 1.2.2, each electrode was investigated and various appropriate electrolytes for each electrode were tested. In total, seven electrode systems were investigated using three solid electrodes in combination with mercury and bismuth films (Figure 12). All the parameters and solutions were the same for each of these comparisons.

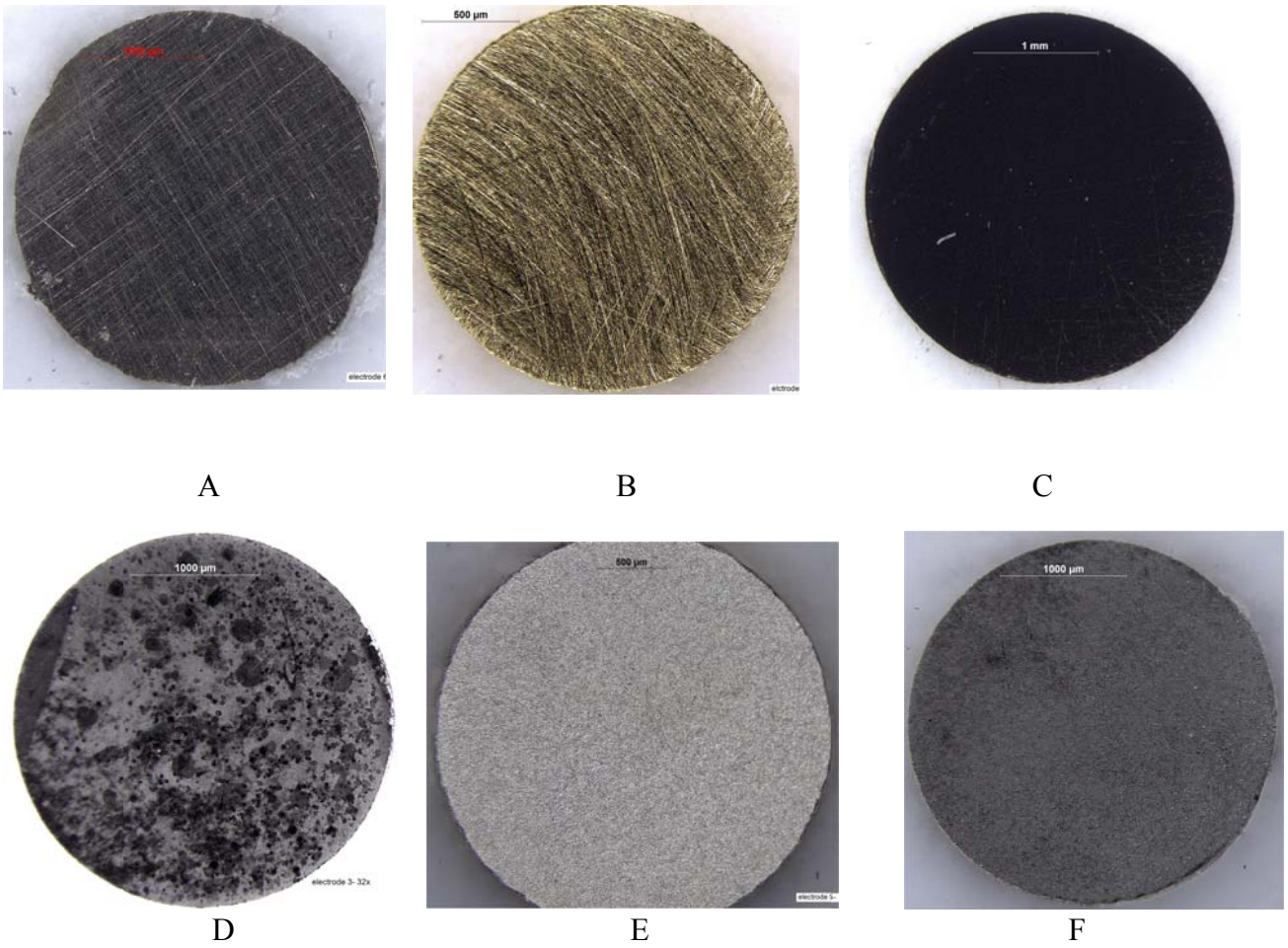

Figure 12. Solid electrode surfaces photographed using *Leica* microscope; [A] – solid bismuth electrode (BiE), [B] – solid gold electrode (Au) employed bare and with *in-situ* Hg, [C] – glassy carbon electrode (GCE) combined with *in-situ* Hg, [D] – glassy carbon electrode with bismuth film, [E] – solid gold electrode with mercury film and [F] – glassy carbon electrode with mercury film.

3.3.1 ELECTRODE CONDITIONING

Voltammetric studies [*16, 36*] have reported the need to condition the electrode surface when bare electrodes are used in order to activate the electrode for the successful deposition of the required analyte. Conditioning of the electrode means that the electrode is held at a particular potential in a specific electrolyte, usually acidic, for a fixed time or a high concentration of the analyte of interest is run in multiple runs, approximately 10 runs, to 'activate' the electrode. Researchers are still trying to understand what exactly happens to the electrode surface during this conditioning step, current understanding is that the electrode is oxidized and also any contamination such as organics for example, are being removed during that process.

No work has been published on the effect of conditioning of glassy carbon electrode or any other electrode for the deposition of barium. Therefore this study looked at the effect of conditioning on the deposition of barium for bare solid electrodes: gold, glassy carbon and bismuth. It was found that the bare gold electrode was unable to detect barium even after multiple conditioning runs using Ba concentrations up to 1ppm and various electrolyte concentrations between 0.01 M and 1.0 M. Pascal's (*16*) successful work with gold electrodes for the detection of antimony and other metal ions provided some merit in trialing the gold electrode for barium, however, the lack of success with barium could be due to the fact that Pascal used acidic electrolytes. In this work it was not possible to use acidic electrolytes due to the highly negative deposition potential (Figure 13A). In contrast, a bare bismuth electrode detected barium after a few conditioning runs but the peak was large and rounded and not sharp and well resolved (Figures 13B and 13C).

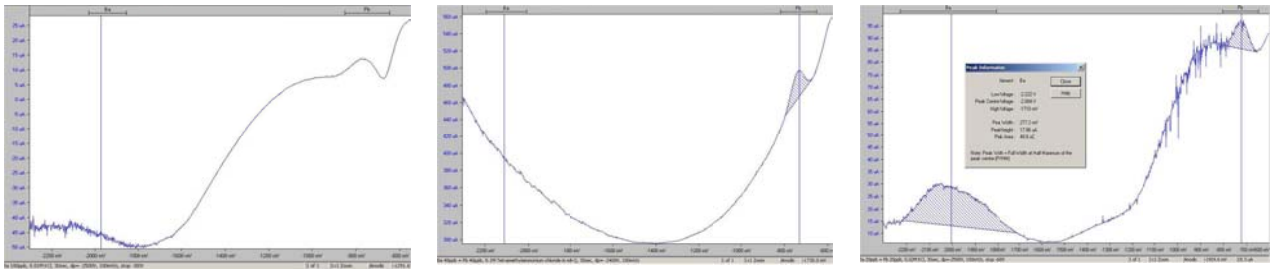

A B C

Figure 13. Voltammograms of working electrodes in KCl electrolyte: [A] bare Au electrode (Ba 100 ppb), [B] bare Bi electrode before conditioning and [C] bare Bi electrode (Ba 20 ppb) after two conditioning runs.

Conditioning for the glassy carbon electrode was variable and typically required two to ten runs after polishing on the Buehler pad. Further conditioning was required again after performing several voltammetric runs or after running acidic samples (Figure 14A & 14B).

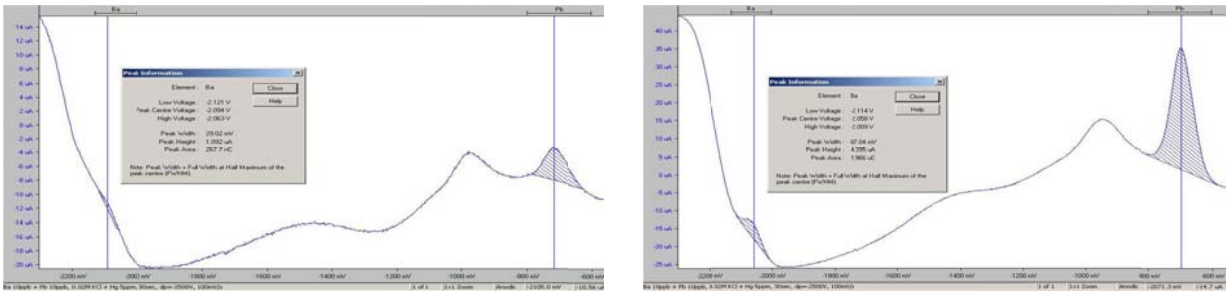

A B

Figure 14. Voltammograms of GC working electrodes in KCl electrolyte: [A**]** pre-conditioning (Ba 10 ppb + Pb 10 ppb), [B] post-conditioning **(**Ba 10 ppb + Pb 10 ppb). The Ba peak is seen at -2058 mV and the Pb peak at -750 mV.

This study also found that polishing the glassy carbon electrode was also required apart from the conditioning, since the 'smoothness' of the electrode surface significantly affected the sensitivity of the electrode towards the analyte, as illustrated in Figures 15A and 15B. The barium analyte peaks were only detected after re-polishing the glassy carbon electrode once the surface had been contaminated or scratched. This agrees with other studies that showed a smooth electrode surface was important to ensure a uniform deposition of films [*36*].

A

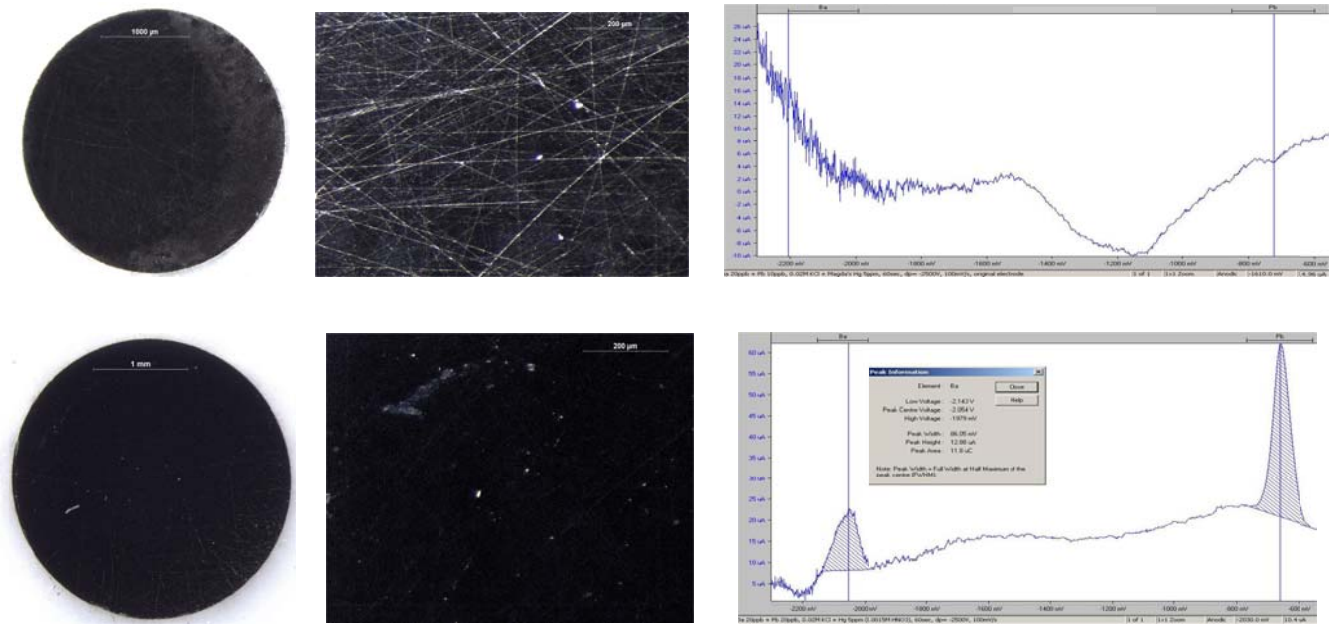

B

Figure 15. The surface of the glassy carbon electrode as seen through a microscope [A] after harsh polishing with fine grit sandpaper, and [B] re-polished correctly. The scratched surface of the electrode in [A] is clearly visible. The photographs in the middle are close-ups of the electrode surfaces shown on the left. Voltammograms depicting the electrode outputs associated with each are on the right.

3.3.2 SOLID GOLD ELECTRODE

A number of runs at various deposition potentials were attempted using bare Au electrode in 0.1 M KCl electrolyte, however, it was not possible to detect barium even at very high concentrations, as shown in (Figure 13 A). Other electrolytes were also trialed without any success. As stated previously, Pascal's [*16*] work with gold electrode merited trialing this electrode for barium detection, however it became apparent that the electrolyte used for barium detection was not appropriate for the gold electrode. More acidic electrolytes cannot be used for barium detection due to excessive gas formation. Therefore, the bare, solid gold electrode was not considered suitable for barium detection.

3.3.3 SOLID GOLD ELECTRODE WITH MERCURY IN-SITU

Although the bare gold electrode was not successful but because gold has high affinity for mercury, that is, it forms an amalgam, and the fact that barium has been previously detected using mercury film on glassy carbon electrode, it was decided to trial the gold electrode with *in-situ* Hg in an attempt to co-plate Hg with Ba, and also Pb. Pb was detected with this system but a Ba peak only appeared at still relatively high concentration of 500 ppb using the previously chosen parameters and was very small and poorly resolved at 1.5 µA (Figure 16). The Ba peak was also not reproducible and was not visible after three analytical runs.

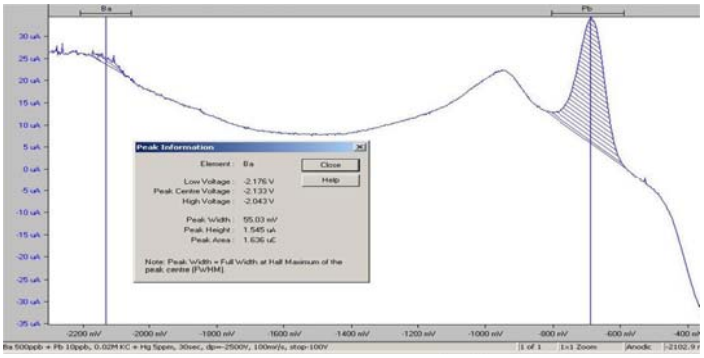

Figure 16. Capacitance peaks for Ba 500 ppb and Pb 10 ppb on Au- *in-situ* Hg electrode system.

3.3.4 SOLID GOLD ELECTRODE WITH MERCURY FILM

Following the Au-Hg *in*-situ investigation, which revealed that Ba could be detected at high concentrations, but not reproducibly, the use of Au-Hg film electrode system was trialed. Since previous studies using glassy carbon electrode struggled with keeping the mercury film on the surface of the electrode when a deposition potential of -3000mV was applied, if an amalgam with gold was formed, that might provide a much more robust mercury film, which ideally would not be stripped off at high negative potential. A thick mercury film was required to ensure that the entire electrode surface was covered to prevent unwanted reactions occurring with any exposed gold on

the surface of the electrode [*41*]. The thick Hg film used on the Au electrode was indeed found to be very robust. Once plated on, it could not be removed without sanding the electrode surface back to fresh gold. Despite having a robust mercury film, unfortunately the sensitivity towards Ba was still very low, producing a mean response of 2.28 ± 0.37 µA for Ba concentration of 20 ppb for 30sec deposition time and only up to 11.98 ± 1.08 µA for 100 ppb Ba. When compared to Pb for example, the peak height for 20 ppb Pb on Hg film was around 40 µA, which is 20 times as sensitive. The barium peaks were consistent however, and peak heights displayed good linearity in the range from 20 – 100 ppb in KCl electrolyte (Figure 17). Thus, despite the success of being able to detect barium consistently and with good linearity, with this system, the low sensitivity means that it would not be possible to use this system for real samples, such as GSR samples, where large dilution is required due to the high acidity of these samples.

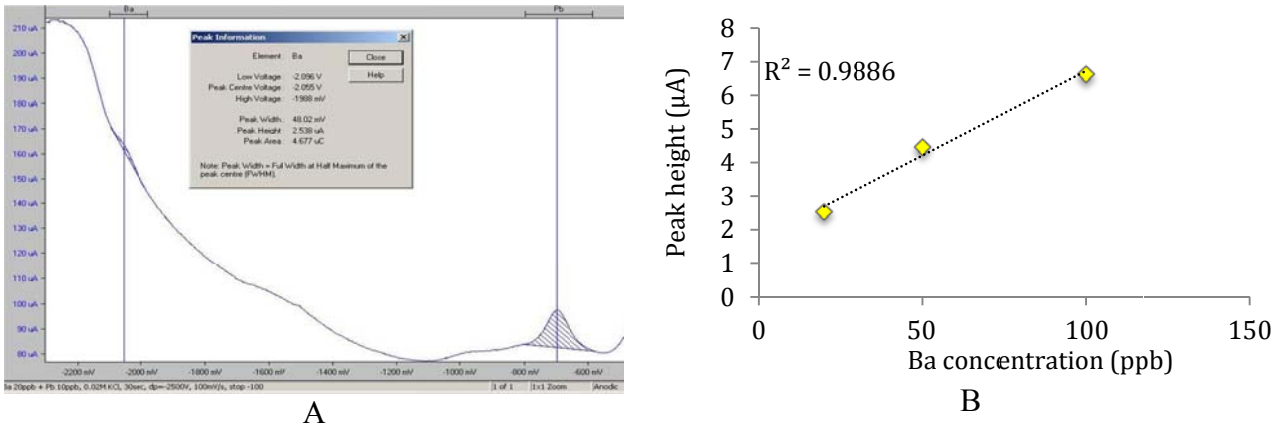

A B

Figure 17. [A] Voltammogram showing Ba peak height of 2.58 µA at -2055 mV and Pb peak at -700 mV on the right, [B] linear range for Ba 20 – 100 ppb using Au-Hg film electrode (r^2 = 0.988).

3.3.5 GLASSY CARBON ELECTRODE WITH MERCURY FILM

The GCE/mercury film electrode system has been used for previous work with barium [*18, 23, 22*]. One major issue with this system is the loss of mercury film during voltammetric runs. A thicker film (by depositing mercury for longer, up to 10 minutes and using higher Hg concentration in the matrix, up to 500 ppm, as normally a 5 minute deposition is used with 20 ppm concentration) was trialed but with the same outcome. Whether using thin or thick *ex-situ* deposited Hg film, it deteriorated after several runs and produced inconsistent peak heights for Ba in KCl electrolyte (Figure 18), probably due to lack of deoxygenation of the solution prior to analysis in this work. Woolever and Dewald [*18, 22*] used $LiClO_4$ and organic electrolytes such as tetraethylammonium bromide (TEABr) with this working electrode but reported inconsistent results and interference from H_2 evolution. Regular polishing and replating of the film was also required in their work.

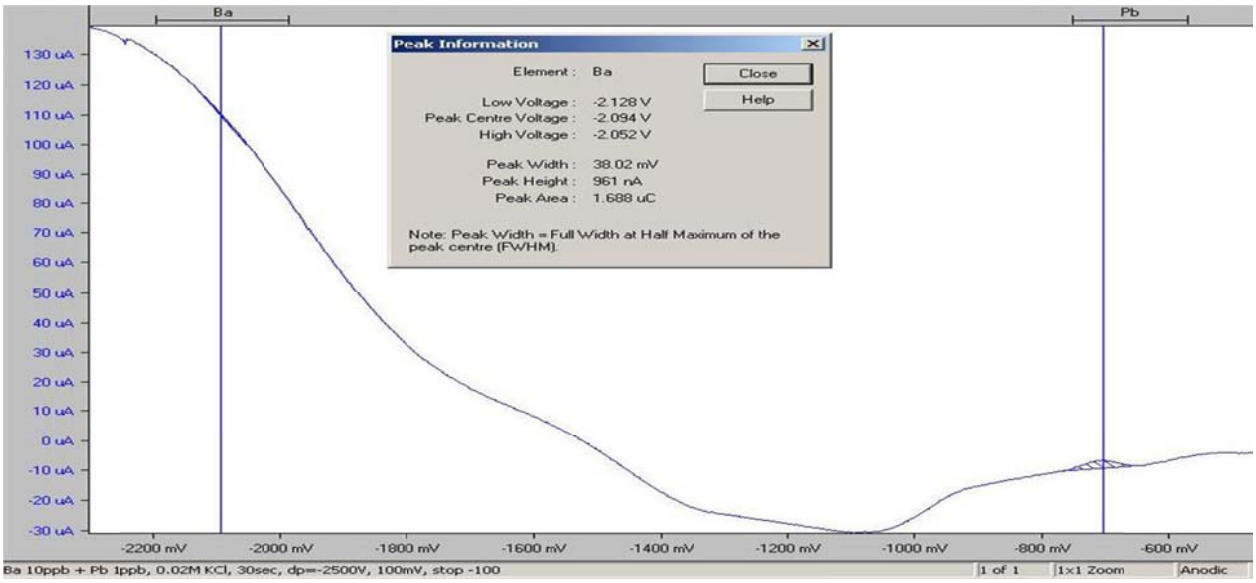

Figure 18. Capacitance peaks for Ba (10 ppb) and Pb (1 ppb) on GCE-Hg film electrode system.

In this study it was observed that an *ex-situ* Hg film could be destroyed on the GCE at very negative potentials. This is most probably due to the ability of Hg to form amalgams with hydrogen and chloride, which could be the cause of the film stripping off the electrode once those species have oxidised. The effect is the same despite the reverse potential scan not running all the way to the Hg stripping potential (+200 mV). Thus, once again, this electrode system was unsuccessful in developing a reliable and reproducible method for the detection of barium which could be applied to various samples, such as GSR and other environmental samples.

3.3.6 GLASSY CARBON ELECTRODE WITH BISMUTH FILM

The glassy carbon/bismuth film system has been studied for Pb, Cd, Zn and other metals [*36*] with successful results. Given the poor results for Hg film and the fact that mercury is hazardous, a Bi film was trialed. This system has not been studied previously, however work by Wang [*26*], has alluded to the possibility of bismuth electrodes being used as an alternative to Hg film electrodes. Like the Hg film however, Bi film deteriorated as quickly as Hg film on carbon. A very small peak of 2.8 µA appeared at -2100 mV for a Ba concentration of 200 ppb (t_{dep} =30 sec), in contrast with the Pb peak of 66 µA (t_{dep} = 30 sec) at -700 mV for only 10 ppb concentration (Figure 19).

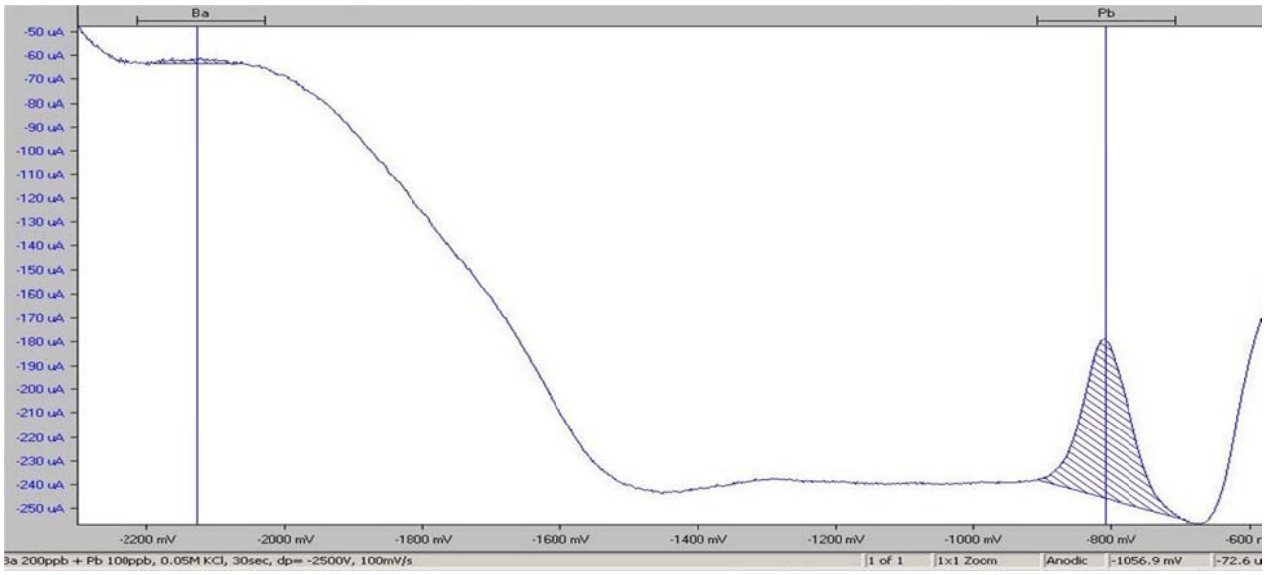

Figure 19. Capacitance peaks for Ba (200 ppb) and Pb (10 ppb) on GCE-Bi film electrode system.

The bismuth film also stripped 'earlier' than -300 mV depending on the electrolyte, and interfered with Pb peaks. The Bi film oxidised at approximately -300 mV or even -700 mV depending on the type and pH of the electrolyte, limiting the width of the window. This restricts the ability to see a Pb peak, for example, if it has shifted to a much less negative position than its typical stripping area of -800 mV. Furthermore, at very negative potentials the film deteriorated in much the same way as Hg, even when the Stop Measurement Potential remained at -1200 mV in order not to reach the Bi stripping point. It was surprising that Bi film did not work, given bismuth's similar properties to mercury and success of Bi film with voltammetric analysis of other metals published in the literature [*26*].

3.3.7 SOLID BISMUTH ELECTRODE

Given that barium was detected with bismuth film, though not sensitively, the solid bismuth electrode was trialed next to eliminate the issue of deterioration of the bismuth film. The following electrolytes were investigated for this electrode: KCl, TMACl, ClAc, HNO_3 and ethanoic acid (CH_3COOH). Barium was only detected using TMACl and KCl but sensitivity and peak resolution for Ba in both TMACl and KCl was poor in both electrolytes. TMACl and KCl were pH 5 – 6, closer to neutral than the other acidic electrolytes. Electrolyte concentrations ranging from 0.01 M – 1.0 M TMACl, and 0.01 M – 0.05 M KCl were trialed.

In 0.1 M TMACl for Ba concentration of 50 ppb, the peak height was 11.8 µA after t_{dep} of 30 sec and best resolved at a deposition potential of -2500 mV, as shown in Table 3, where less negative potentials (ie. -2200 mV) were not negative enough for the deposition of barium on bismuth electrode and more negative potentials (ie. -2700 mV) generated too much gas, which interfered with barium detection.

Table 3. Effect of deposition potential on sensitivity of Bi electrode to 50 ppb barium.

Electrolyte	Ba Peak Height (µA)					
Deposition potential (mV)	-2200	-2300	-2400	-2500	-2600	-2700
0.1M TMAC	-	-	9.95	11.8	4.41	-
0.02M KCl	-	-	-	2.19		-

In 0.02 M KCl, the peak current generated after t_{dep} of 60 sec for 100 ppb Ba was 3.49 µA at -2066 mV but as illustrated in Figure 20 A, the shape was broad and rounded, not sharp and well resolved like the Pb and Bi peaks present at -800 mV and -600 mV respectively. The same Ba concentration produced a 21.5 µA peak after t_{dep} of 60 s in TMACl using identical parameters (Figure 20 B). One issue was the extreme noise generated at approximately -700 mV, near the Pb stripping peak, which worsened over analytical runs. This was suspected to be the BiE itself, stripping earlier than expected in the chosen electrolytes. In TMACl electrolyte, addition of HNO_3 increased noise and peaks became misshapen and Pb stripping peaks shifted more positively to -400 mV.

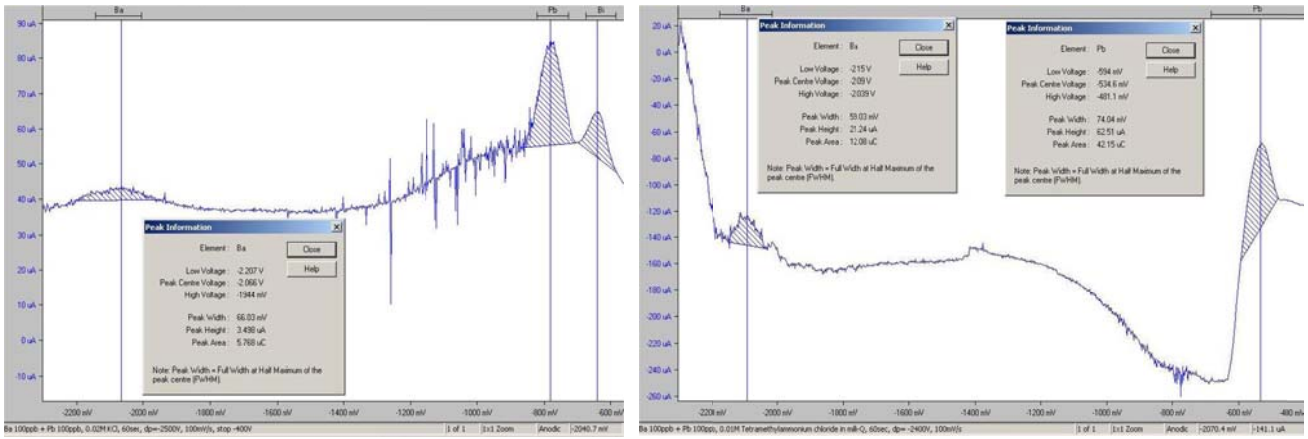

A B

Figure 20. Capacitance peaks after t_{dep} of 60 sec at dp = -2500 mV for Ba 100 ppb and Pb 100 ppb generated using bismuth electrode in [A] 0.02M KCl and in [B] 0.1M TMACl.

The round, flattened capacitance peak produced for Ba in KCl compared with the Pb and probable Bi peaks seen in Figure 20 A, may have been influenced by the sweep rate as Wu found for Cu and Pb [35]. If the reaction rates for Ba are much slower than for Pb, like Wu found for Cu, then using a slower sweep rate may improve the peak resolution.

The bismuth electrode has shown some promise with regard to barium detection. It is an attractive alternative to using mercury film and it eliminates the need for barium film formation, however, the sensitivity is still not as good when compared with the GCE + *in-situ* Hg system (see Section 3.3.8). Unfortunately, due to the fact that the aim of this work was to develop a method for the detection of barium in samples that may be highly acidic and thus would require significant dilution, the method needs to be able to detect low concentrations of barium, ideally down to 10ppb. The bismuth electrode was therefore not ideal.

3.3.8 GLASSY CARBON ELECTRODE WITH MERCURY IN-SITU

Previous investigation (see Section 3.3.5) with Hg film on glassy carbon electrode showed that Ba can be easily detected if the mercury film is present, therefore, it was decided to test co-deposition of mercury with barium, by placing high concentrations (ppm levels) of mercury into electrolyte. Similar work was done previously by Vuti *et al.* [*30*]. Having 5ppm Hg in solution, which is the concentration used for plating the *ex-situ* film onto the electrode, resulted in a clear, resolved Ba peak visible on the voltammogram in addition to a peak for Pb (Figure 21).

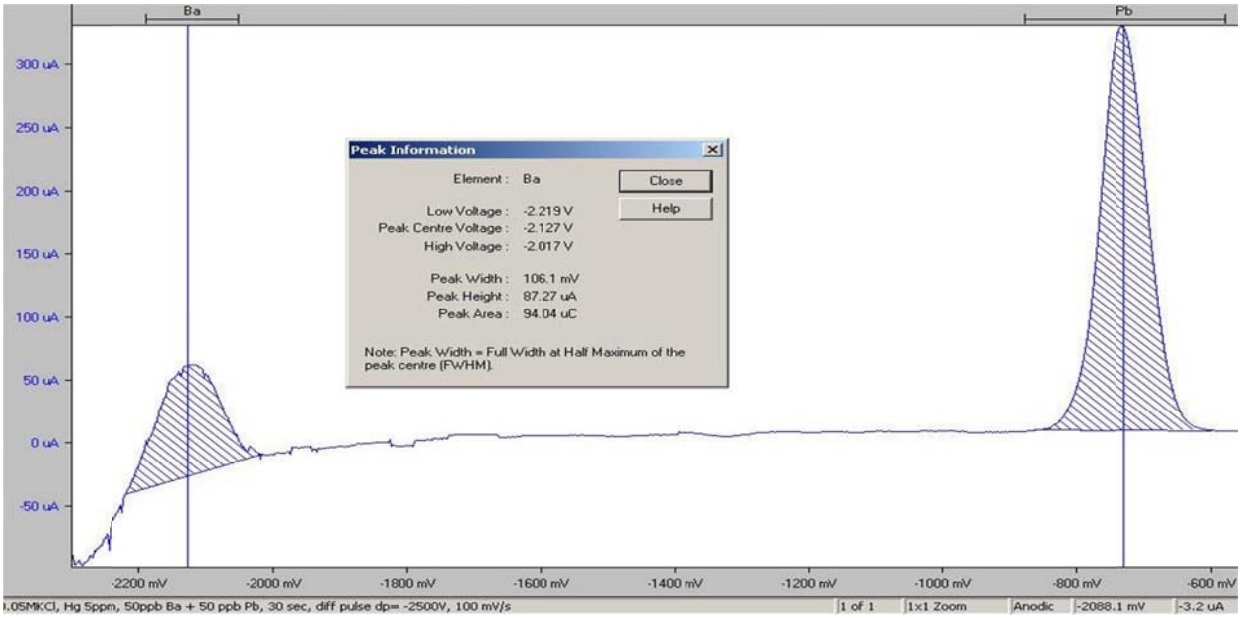

Figure 21. Capacitance peaks produced after t_{dep} of 30 sec for Ba (50 ppb) and Pb (50 ppb) in 0.05 M KCl at dp = -2500 mV, 100 mV/s on the GCE-*in-situ* Hg electrode system.

After a number of runs, a thin Hg film was visible on the electrode surface. Interestingly, this is probably a net result of Hg forming amalgams that assist Ba and Pb in deposition, but then is not oxidized itself as the analyte metals oxidise and strip off at their more negative stripping peak areas. This thin film required removal periodically, because of the Pb and Ba amalgams formed within it that caused capacitance peaks to appear in the blank. This observation is supported in Vuti *et al.*

[*30*], where *in-situ* Hg on glassy carbon was used in conjunction with $LiClO_4$ and cyclic-square wave voltammetry to detect an organic GSR component with Ba in one run. As shown in Table 4, the GCE + *in-situ* Hg performed best overall. BiE produced similar peak heights to GCE + *in-situ* Hg, but peak resolution was poor and variability was high between replicates.

Table 4. Comparison of barium peak heights from three electrode systems under the same conditions for 20 ppb barium: 0.02 M KCl, t_{dep} = 30 sec, dp = -2500 mV, 100 mV/s.

	Ba Peak Heights (μA)		
t_{dep} = 30sec (n = 10)	GCE + *in-situ* Hg 5ppm	Au + Hg film	Solid BiE
Mean	19.08	2.28	17.44
Std. dev.	1.121	0.37	2.04
%RSD	5.87	16.2	11.69

Comparing all the successful systems, the most reliable in terms of reproducibility and most sensitive towards barium was the glassy carbon electrode with in-situ mercury in potassium chloride electrolyte. This system was then further optimized as discussed in Section 3.4.

3.4 OPTIMISATION OF THE BEST SYSTEM: GLASSY CARBON ELECTRODE WITH MERCURY IN-SITU

Having determined the best electrode system, optimisation of the electrolyte was the next step for this system. The three key components of the electrolyte matrix that required investigation were: concentration of the bulk electrolyte, mercury concentration and nitric acid concentration from the barium and mercury standards.

Having trialed TMACl, ClAc, HNO_3, CH_3COOH and KCl during electrode investigation, the preferred electrolyte was found to be KCl, due to its more neutral pH, low toxicity and generally flatter baseline. Optimisation of the KCl concentration was carried out by using a low concentration of Ba (10 ppb) in the minimum concentration of electrolyte (0.01 M) and increasing concentration stepwise by 0.01 M up to a maximum of 0.1 M KCl (Table 5). Three replicates at each concentration level were taken with a blank run performed at each concentration change. The response for Ba was unexpectedly varied and non-linear, ranging from a mean value of 14.25 ± 2.23 μA for 0.01 M KCl, to 2.40 ± 1.19 μA for 0.05 M KCl, to 6.78 ± 0.96 μA for 0.1M KCl concentrations.

Table 5. Change in response of Ba (10 ppb) as KCl concentration is increased from 0.01 M to 0.1 M, Hg 5 ppm, t_{dep}= 60 sec, dp= -2500 mV, 100 mV/s, differential pulse. Yellow highlighted values are considered optimal due to substantial peak height and lower standard deviation between replicates than at other concentrations of KCl.

	Ba 10 ppb (µA)	
KCl concentration (M)	Mean ± std deviation (n = 3)	% RSD
0.01	14.25 ± 2.23	15.6
0.02	13.45 ± 0.55	4.1
0.03	6.46 ± 0.67	10.4
0.04	2.72 ± 0.46	16.9
0.05	2.40 ± 1.19	49.6
0.06	3.27 ± 0.67	20.5
0.07	5.56 ± 2.25	40.5
0.08	7.37 ± 1.38	18.7
0.09	5.68 ± 1.39	24.5
0.10	6.78 ± 0.96	14.2

Repeating the experiment yielded the same variable results, which may be due to the use of electrolyte concentrations < 0.1 M when the accepted rate constants for the electrode/electrolyte electron transfer reactions do not apply [*34*]. Higher concentrations of ≥ 0.1 M were not investigated here because obvious gas evolution with strong odours occurred at these higher concentrations which resulted in excessive baseline noise obscuring the Ba peak after a few runs. Within the concentration range investigated, 0.02 M KCl behaved most reliably and was chosen as the optimum concentration for this method.

3.4.1 INVESTIGATION OF MERCURY CONCENTRATION

Barium was much more easily and consistently detected with mercury, a generally accepted conclusion supported by Wang [*19, 30*] and others, but the optimum concentration for *in-situ* use was not clearly established in the literature. Princeton Applied Research [*37*] recommends 2.5 – 5 ppm $Hg(NO_3)_2$ directly added to the sample solution.

The GCE was used to examine the effect of *in-situ* Hg concentration on peak heights obtained using 10 ppb and 50 ppb Ba standard concentrations (Figure 22). Peak heights were diminished at 1 ppm Hg compared with the use of 5 ppm Hg, but heights were even more adversely affected by the addition of 10 ppm Hg. The difference in response seen was larger with a greater concentration of analyte. The reasons for this are not clear, however, it is possibly due to the increase in Hg ions outcompeting Ba for sites on the finite surface area of the electrode, which limits the quantity of ions that can be adsorbed [*24*]. Consequently, the optimum Hg concentration was found to be 5 ppm for both low and high barium concentrations.

Figure 22 displays the deterioration of peak heights as increasing quantities of Hg standard are introduced to the electrolyte, and so 5 ppm *in-situ* Hg was selected as the optimum concentration based on this investigation.

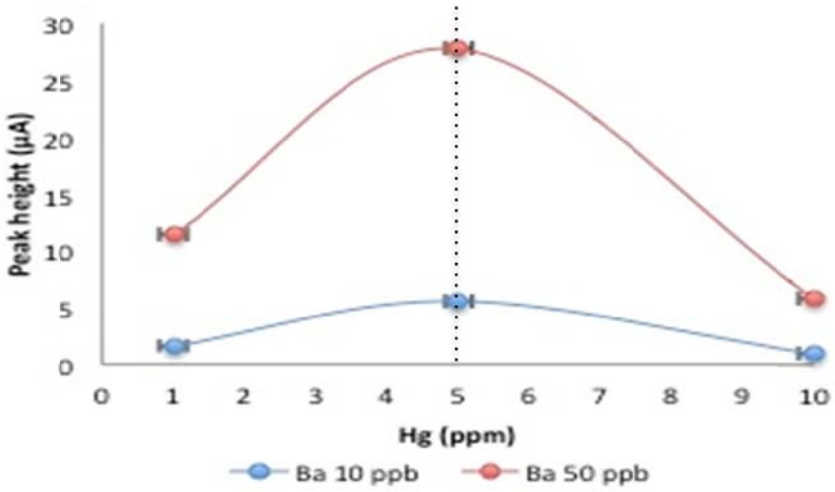

Figure 22. Mean peak heights for Ba obtained during voltammetric analyses with varying concentrations of mercury. The dotted line indicates the optimum concentration of Hg in-situ.

3.4.2 INVESTIGATION OF NITRIC ACID CONCENTRATION

The potassium chloride (KCl) plus *in-situ* mercury (Hg) electrolyte should properly be termed the KCl/Hg/HNO_3 electrolyte, as the addition of Hg and any analyte standard involves the introduction of the matrix solution in which those elements are dissolved. In this case, the matrix solution was dilute nitric acid (HNO_3). Research indicates that KCl is never run 'alone' for this method as it is always combined with Hg *in-situ* in order to facilitate the co-plating of analyte metals onto the working electrode [*22, 30*]. The concentration of nitric acid in the Hg, Ba and Pb standards also needs to be included as a source and their quantities calculated. The purpose of investigating the effect of nitric acid, therefore, was to determine the tolerance level of this method for nitric acid in the matrix, recommended in Woolever and Dewald [*18, 22*] in anticipation of sample analysis.

Addition of acid was investigated because of the tendency for H^+ ions in solution to reduce to H_2 gas during the stripping process in ASV. In an effort to reduce the evolution of gases, that is, Cl_2 and H_2, the lowest KCl concentrations were investigated that would still support conductivity and trace level Ba^{2+} ions, along with the maximum amount of nitric acid that would simulate the addition of sample solution (Table 6). For 0.02 M KCl, peak heights for Ba (50 ppb) ranged from 5.86 ± 0.11 µA to 16.99 ± 1.2 µA and down to 4.99 ± 0.29 µA in corresponding HNO_3 concentrations of 0.00156 M, 0.00256 M and 0.01006 M. At this stage, lead was also investigated, keeping in mind the application of this method for GSR sample analysis. The respective Pb peaks were 50.07 ± 5.39 µA and 76.62 ± 10.5 µA, but no peak height for 0.01006 M HNO_3 due to peak shifting effects from the change in electrolyte composition. Pb peak heights were more variable between replicates than Ba peak height values. Ba peak heights were reduced in 0.01 M KCl for the same HNO_3 conditions ranging from 2.51 ± 0.52 µA to 1.43 ± 0.38 µA up to 5.84 ± 0.27 µA and similarly reduced for Pb at 43.42 ± 1.05 µA, 34.8 ± 0.55 µA and 34.35 ± 7.54 µA; and peak height data was not discernible for Ba or Pb when KCl concentration of 0.001 M was tested.

Table 6. Glassy carbon electrode, investigation of nitric acid effects, using 0.01 M / 0.02 M KCl + Hg 5 ppm (0.0015 M HNO_3), Ba 50 ppb + Pb 50 ppb (total 0.00006 M HNO_3), 30 sec, dp = -2400 mV, 100 mV/s. Optimum concentrations of KCl / HNO_3 is highlighted in yellow.

Electrolyte concentration (M)	Initial HNO_3 concentration including Hg and metal standards (M)	Additional volume of 3% HNO_3 (µL)	Total HNO_3 concentration including Hg and metal standards (M)	pH	Ba mean ± sd (µA) (n = 3)	Pb mean ± sd (µA) (n = 3)
0.001	0.00156	0	0.00156	2.8	-	-
	0.00156	40	0.00256	2.6	-	-
	0.00156	200	0.01006	2.0	-	-
0.01	0.00156	0	0.00156	2.8	2.51 ± 0.52	43.42 ± 1.05
	0.00156	40	0.00256	2.6	1.43 ± 0.38	34.80 ± 0.55
	0.00156	200	0.01006	2.0	5.84 ± 0.27	34.35 ± 7.54
0.02	0.00156	0	0.00156	2.8	5.86 ± 0.11	50.07 ± 5.39
	0.00156	40	0.00256	2.6	16.99 ± 1.20	76.62 ± 10.50
	0.00156	100	0.00506	2.3	1.50 ± 0.08	25.07 ± 7.29
	0.00156	200	0.01006	2.0	4.99 ± 0.29	-

During this study, the volume of 0.001 M HNO_3 added to the KCl electrolyte as a sample proxy was 40 µL (3% HNO_3) but this would equate to 63 µL for a real sample, since most samples are acidified with 2% HNO_3. 100 µL of real-world sample therefore, would be equal to an additional ~ 0.0015 M HNO_3 in the electrolyte solution, bringing the combined total to 0.003 M HNO_3 (3.0 mM) prior to standard additions.

When total concentration of HNO_3 reaches 0.005 M both Ba and Pb peaks reduce significantly, due to gas formation during the stripping step, as shown in Table 6. Above 0.005 M HNO_3 concentration, the Pb peaks shift out of range of the detection window. An appropriate volume of acidified sample would therefore be < 100 µL, based on the data.

3.5 METHOD VALIDATION

As a result of the investigations, the optimised method for barium detection, including the simultaneous detection of lead, was found to be the glassy carbon electrode with *in-situ* Hg 5 ppm combined with 0.02 M potassium chloride electrolyte with less than 3.0 mM HNO_3 content. The optimal voltammetric parameters were: differential pulse potential delivery at 100 mV/s, with pulse height of 50 mV and step duration of 10 ms; deposition potential of -2500 mV with t_{dep} of 30 seconds, and measurement start and stop potentials from -2300 mV to -500 mV within a range of 3 mA.

Validation of an analytical method is the procedure used in laboratory studies to evaluate the performance of a newly developed method [*40*]. The developed method must meet the requirements for the intended analytical applications. The constituents of method validation are: linearity range, limit of detection, accuracy, precision, and selectivity. The following Section contains the figures of merit for the validation of this method.

3.5.1 LINEAR WORKING RANGE

The linear response for barium using *in-situ* Hg on glassy carbon was better than on any other electrode/electrolyte system investigated. For parameters of 0.02 M KCl + Hg 5 ppm, dp= -2500 mV, 100 mV/s and a deposition time of 30 sec, the linear range was determined to be 10 - 160 ppb (Figure 23). If the deposition time was increased then the linear range was decreased and the same time the limit of detection was lower.

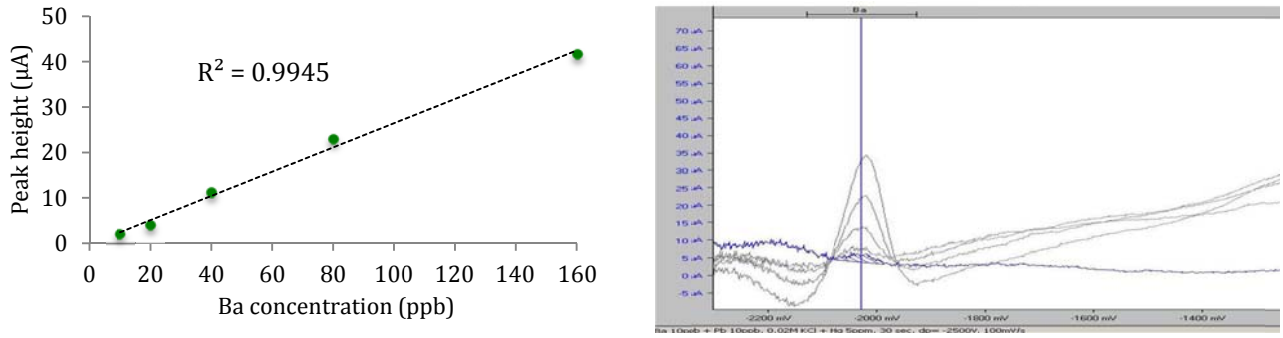

Figure 23. [A] Linear range from 10 - 160 ppb ($r^2 = 0.994$) for GCE using parameters of 0.02 M KCl + Hg 5 ppm (0.0015 M HNO_3), t_{dep}= 30 sec, dp= -2400 mV, 100 mV/s. Ba 10 – 160 ppb. [B] Superimposed voltammograms from A showing increasing Ba concentrations.

Linearity also needed to be tested after the introduction of nitric acid as a sample proxy and it actually improved, although the range decreased (Figure 24). As expected, a longer deposition time reduced the range as the accumulation of analyte saturated the electrode; peak heights also approximately doubled in value.

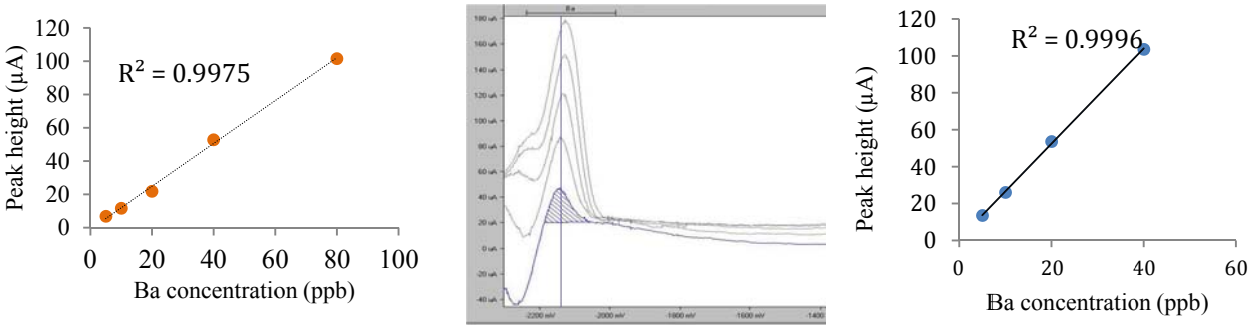

Figure 24. [A] Linear range from 5 - 80 ppb ($r^2 = 0.997$) for GCE, 0.02 M KCl electrolyte + Hg 5 ppm (0.0015 M HNO_3) + 63 µL 3% HNO_3, t_{dep} = 30 sec, dp = -2500 mV, 100 mV/s. [B] Superimposed voltammograms from [A] illustrating linear increase of peaks and [C] linear range from 5 - 40 ppb ($r^2 = 0.999$) for the same parameters as *A* but t_{dep} was increased to 60 sec.

3.5.2 LIMIT OF DETECTION

The limit of detection (LOD) was determined here using a signal to noise ratio of three times the size of the smallest peak above the baseline noise. The peak was approximately 0.5 µA therefore the LOD was considered to be a peak height of 1.5 µA, therefore the limit of detection was 1.55

µg/L (Table 7). The LOD is low enough to allow dilution of samples, minimizing susceptibility of the method to matrix effects, which are effectively diluted out.

Table 7. The response of barium for GCE in 0.02 M KCl electrolyte, t_{dep}= 30 sec, dp= -2500 mV, 100 mV/s, for ten analyses of 20 µg/L Ba concentration.

Run	GCE + *in-situ* Hg 5ppm Ba (µA)
1	17.02
2	19.95
3	19.28
4	17.96
5	20.68
6	20.03
7	19.63
8	18.82
9	18.03
10	19.36
Mean	19.08
Std. dev.	1.121
%RSD	5.87
LOD (µg/L)	1.55

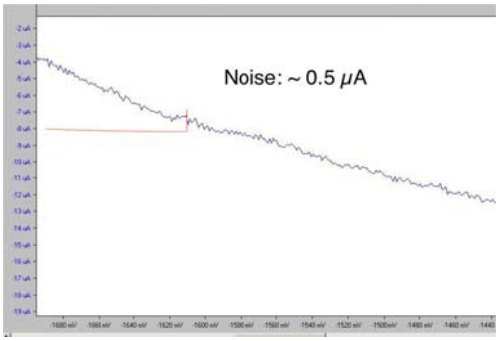

3.5.3 STABILITY

The optimized glassy carbon with mercury in-situ method was used to detect Ba over multiple runs, reliably and reproducibly without the need for deoxygenation of the sample solution, making it ideal for in-field purposes. For 10 measurements performed for Ba concentration of 20 µg/L the mean peak height was 19.08 ± 1.12 µA and a relative standard deviation of 5.87 % (Table 7).

3.6 APPLICATION OF THE OPTIMISED METHOD

Contamination of drinking water with barium has been documented in parts of the USA where barite mine dumps exist and also in the vicinity of gas fracking activities [*6*]. While the threat of barium contamination of Australian drinking water is low, the recent push for gas fracking permits at the State and Federal government level raises flags concerning possible groundwater contamination. Australian drinking water guidelines [*11*] allow a 2 mg/L threshold for barium, which is more than double the 0.7 mg/L threshold permissible in the most recent revision by the World Health Organisation [*12*]. Various types of Western Australian drinking water samples were collected for analysis by voltammetry with the expectation of finding little or no barium in them. In the event of a null result, samples were spiked with Ba standard of known quantity and analysed in

order to verify the feasibility of the method. The samples were tap water, bore water, bottled water and a sample from a rainwater tank. Environmental water samples collected independently from bores in the Pilbara region of Western Australia and previously analysed by ICP-AES were also analysed by the optimised voltammetric method.

3.6.1 DRINKING WATER SAMPLES

Barium content was highly variable between water samples, ranging from 7.59 ± 0.1 µg/L in bottled water, to 73.94 ± 1.57 µg/L in Bullsbrook bore water, and up to 464.56 ± 28.15 µg/L in Wangara bore water (Table 8). Voltammetric analyses were quite variable between sample replicates (see Appendix), RSD being as low as 1.1% and as high as 49.5% across ten samples. None of the concentrations exceeded the WHO guideline threshold of 700 µg/L [*12*]. ASV results were in excellent agreement with ICP-MS data with less than 5% difference as shown in Table 8. An example of a voltammogram for one of the water samples is shown in Figure 26.

Table 8. Total Ba concentrations determined in 10 drinking water samples, taken from municipal tap water, bores, a rainwater tank and bottled water.

	Barium Concentration (ppb)					
Sample	ASV Mean (µg/L) (n = 3)	Std. deviation	%RSD	Range (µg/L)	ICP-MS (µg/L)	% difference
Bottled water, Mt Franklin brand	7.59	± 0.10	1.3	7.49 – 7.69	7.1	3.34
Rainwater, Muchea tank	8.47	± 1.29	15.23	7.18 – 9.76	9.5	5.73
Drinking fountain water, ECU	429.73	± 26.39	6.1	403.34 – 456.12	430	0.03
Tap water, Wanneroo residence	411.2	± 30.0	7.29	381.2 – 441.2	419	0.94
Filtered tap water, Wanneroo (Waterways USA)	419.76	± 4.41	1.1	415.35 – 424.17	420	0.03
Bore, Windsor Rd Wangara	464.56	± 28.15	6.1	436.41 – 492.71	460	0.49
Bore, Chittering Rd Bullsbrook	75.22	± 37.25	49.5	37.97 – 112.47	72	2.19
Bore, Jenkins Rd Bullsbrook	73.94	± 1.57	2.1	72.37 – 75.51	71	2.03
Bore, Craigie	60.89	± 6.53	10.72	54.36 – 67.42	60	0.74
Bore, 85m Muchea	48.74	± 7.99	16.4	40.75 – 56.73	48	0.76

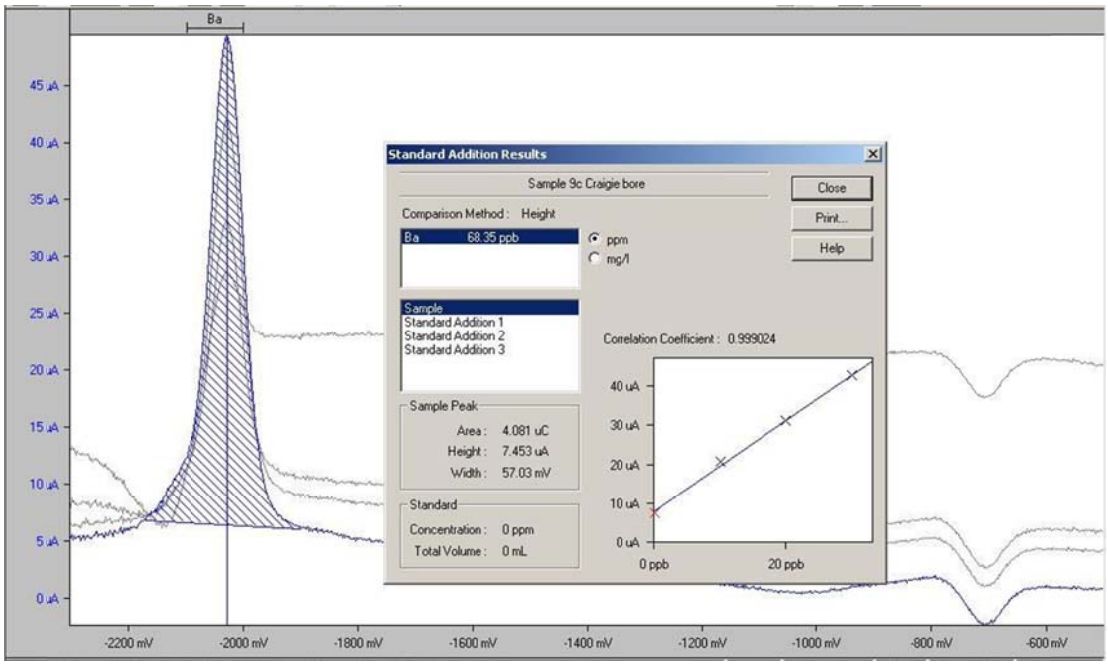

Figure 26. Standard addition voltammogram of barium response in the Craigie bore water sample, using glassy carbon (GCE) electrode in 0.02 M KCl electrolyte, t_{dep}= 30 sec, dp= -2500 mV, 100 mV/s.

The dilution factor used for each sample may have had some effect on the RSD. The bottled water and rainwater samples did not require dilution for example and contained similar Ba content, but an unidentified element in the rainwater (most probably organic) affected the Ba peak height with each run. Another interesting example is the unfiltered tap water versus the filtered tap water and ECU drinking fountain water. The RSD for tap water was 7.29 % and 6 % for the ECU fountain water compared with 1.1 % for the filtered tap water. This indicates that unidentified elements in the unfiltered water were probably affecting the accuracy of the voltammetric analysis which filtering removed from the tap water sample, but was possibly not filtered out in the ECU drinking fountain water.

The drinking water samples revealed some interference at the barium stripping region in the bore water and tap water samples compared with rainwater and bottled water. Some Ba peaks were slightly shifted or peaks became part of a large 'shoulder' making it more difficult to distinguish from the baseline. The presence of high alkalinity or calcium content in those samples could be the cause or suppressive effects from other metals not accounted for in the ICP-MS analysis, and is in agreement with effects reported by Wang *et al.* [*15*] during ASV studies on alkaline earth metals, particularly for calcium and barium.

Results for barium concentrations in natural water samples were expected to be low because Australian geology is not a prime source of barite deposits, unlike the UK and USA where much

mining is done [*4, 6*]. Interestingly, the municipal water sources were much higher in barium together with one bore from a residence located near an urban industrial park, than the water from bores outside the Perth metropolitan area. It is not clear whether the increased barium content is from the water sources that comprise municipal supply or from the water treatment processes that are applied before release into the community, but the concentration is well within the acceptable range for Australian drinking water [*11*]. The residential tap water actually increased in barium content after filtration with a Waterways countertop filter cartridge (Table 8), but this may have been due to suppression of the barium signal due to other ions present in the unfiltered water, that were subsequently removed by the ion exchange process in the cartridge.

3.6.2 ENVIRONMENTAL SAMPLES

Bore waters collected in the Pilbara region were obtained from ChemCentre, the samples contained Ba concentrations in the range from 40 – 280 μg/L as determined by ICP-AES analysis (Table 9). Due to the fact that these samples were acidified, only two samples had high enough concentrations to allow for voltammetric analysis. The barium concentrations present in the rest of the samples were such that a dilution factor of more than 10x produced trace amounts within the diluted sample that were at the LOD for the method. Also due to time constraints each sample was only analysed once, therefore accurate data was not obtained. However, despite that, it was possible to detect barium in those two samples and the ASV results were well within acceptable % error range, with one sample giving less than 1% difference and the other 5.8% difference with the ICP-MS result.

Table 9. Total Ba concentrations determined in two environmental water samples, taken from groundwater bores and reticulation systems.

	Barium Concentration		
Sample	ASV (μg/L)	ICP-AES (μg/L)	% difference
1	96.4	95	0.7%
2	314.4	280	5.8%

Interestingly, barium concentrations in the Pilbara bore waters were very similar to those found in the Perth area water samples, which reinforces the stated geological dearth of barite deposits in Australia.

3.6.3 BRAKE PAD DUST SAMPLES

Most of the brake pad dust samples contained very high amounts of Ba, so even though the samples were acidified to extract the metals, such low sample quantities were required that any matrix

interferences were negligible during the voltammetric analyses. Ba concentrations determined by ASV analysis and ICP-MS are given in Table 10.

Table 10. Total Ba concentrations determined in five brake pad dust samples, taken from wheel rims, brake calipers and brake pads from cars at a local mechanic's garage.

	Barium Concentration		
Sample	ASV (mg/L)	ICP-MS (mg/L)	% difference
1	14.5	12.0	9.4
2	8.4	8.3	0.6
3	1.6	1.5	3.2
4	2.8	2.7	1.8
5	4.9	4.7	2.1

The ASV results are in excellent agreement with the ICP-MS data, with the largest % difference being less than 10% and smallest less than 1%. Once again due to time constraints these samples were analysed only once, thus, better agreement is to be expected with triplicate runs. These results prove however, that the ASV method developed here for barium detection is robust and accurate enough (as shown in Figure 27) for even these rather complicated matrix samples.

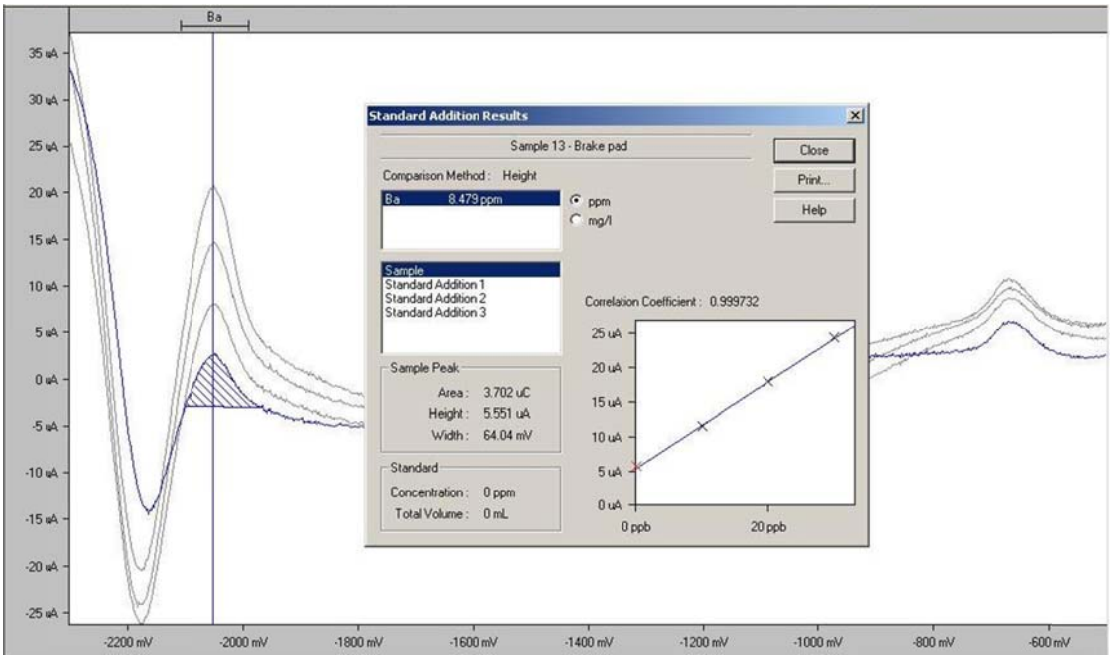

Figure 27. Standard addition voltammogram of barium response in brake pad dust sample, using glassy carbon electrode (GCE) in 0.02 M KCl electrolyte, t_{dep}= 30 sec, dp= -2500 mV, 100 mV/s.

Brake pads have been studied as a source of environmental barium particles but the quantity of barium sulphate contained in the pad, if at all, varies widely between brake pad manufacturers from 0 - 35% [*25*]. This study shows that the barium content in brake dust is in the ppm range, which is high and confirms it is possible to use barium as a tracer for urban particle pollution coming from brake wear [*42*]. For car manufacturers, the quantity of barium determined in dust residues could be an early indicator of deterioration of the brake pads [*25*].

It has been argued that brake pad dust could be mistaken for gunshot residue [*39*], however, this idea is not widely held due to the difference in morphology of the particles revealed by SEM-EDX analysis [*32*]. Thus, using the ASV method at a crime scene to detect the presence of barium in possible GSR samples, would still require the sample to be further analysed by SEM-EDX for particle morphology.

3.6.3 GSR SAMPLES

Gunshot residue is well documented as a source of barium detectable at the site of firearm discharge, [*19*] but its presence and not quantity is the most important factor as an indicator of whether or not a firearm has been used at a site. For this reason, attempts have been made to create a rapid voltammetric screening method to detect Ba, Pb and Sb – the traditional signature metals of GSR, but high variability of analyte concentration and necessary acidification of samples has made this difficult to achieve [*18, 19, 27]*. The optimized ASV method for barium detection developed here was tested on two GSR samples. Due to time constraints only a single analysis was done for each sample. Both barium and lead were detectable in these samples and the results compared to ICP-MS are given in Table 11. The % differences for barium are similar to the environmental and brake pad samples, and well within the acceptable error of less than 10%. However, the Pb result for one of the samples is outside the range of acceptable error. The inaccuracy of this result could be explained by the fact that only a single analysis was performed and the effect of the significant dilution (x100), which was necessary to reduce the acidity of the matrix and any organics present in the sample.

Table 11. Total Ba concentrations determined in two gunshot residue samples.

	Barium Concentration			Lead Concentration		
Sample	ASV (µg/L)	ICP-MS (µg/L)	% difference	ASV (µg/L)	ICP-MS (µg/L)	% difference
1	108.6	97	5.6	71.7	140	32.3
2	91.1	92	0.5	37.8	36	2.4

Both Ba and Pb were simultaneously detected in gunshot residue samples, however Ba concentrations were at the LOD due to necessary dilution of the samples due to acidification during sample preparation. Interferences due to the sample matrix and chemical reactions with Hg are illustrated in the voltammogram shown in Figure 28.

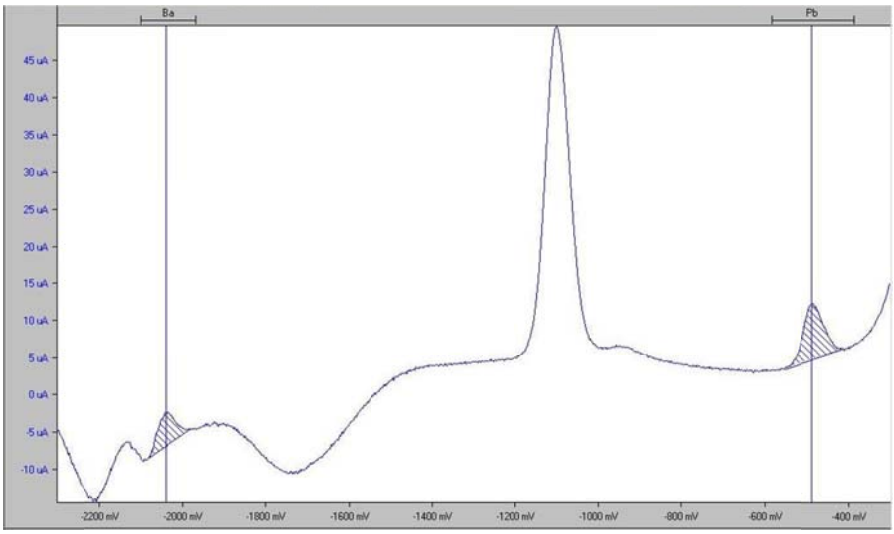

Figure 28. Voltammogram showing simultaneous detection of Ba (shaded peak on the left) and Pb (shaded peak on the right) in a GSR sample using glassy carbon (GCE) electrode in 0.02 M KCl electrolyte, t_{dep}= 30 sec, dp= -2500 mV, 100 mV/s.

Examining the % differences between ASV and ICP-MS data of each individual sample showed considerable variability, which is to be expected, since the two methods of metal ion analysis are different and each is susceptible to different types of interferences and matrix effects. Despite that, overall, the % difference between the two instruments for the various samples studied here is less than 10% for all but one sample. This gives confidence in the ASV barium method developed here, since ICP-MS is the gold standard for trace element detection.

CHAPTER 4 – CONCLUSIONS AND FUTURE WORK

After careful and consistent investigation of various electrodes, electrolytes and optimizing for the most important voltammetric parameters, a robust method for the voltammetric detection of barium in a variety of samples has been successfully developed for in-field application. This is the first time that a reliable, infield voltammetric method for barium analysis has been developed and successfully applied to a variety of samples; drinking water, environmental waters, brake pad dust and GSR.

Key features of the method are the *in-situ* use of mercury, a dilute, non-toxic electrolyte, short duration of analyte accumulation and no deoxygenation of the sample solution being required.

This method was also suitable for the simultaneous detection of Ba and Pb in GSR samples that contain high concentrations of Ba. Samples typically containing high concentrations of Ba such as brake pad dust are best suited to this method as they can be greatly diluted thus removing matrix effects, yet still allow for the detection of barium due to the low limit of detection of this method.

Another advantage of this method is the ability to analyse water samples infield immediately after sample collection without need of acidification.

Despite having developed a successful ASV barium method, there are still a number of limitations to be considered. Firstly, there is a limit to the acidity of the samples being analysed, not less than pH = 2.5; secondly, the method is highly sensitive to any organics present in the sample; thirdly, possible interferences from alkaline earth metals, especially calcium; and finally, the study has also found that barium is highly sensitive to the surface of the electrode and therefore polishing and conditioning of the electrode is required between samples.

Future work in this area should include further investigation into the effect of the surface of the electrode towards barium, especially for bismuth electrode, which showed some promising results as a replacement for mercury, and investigating square wave potential delivery for bismuth, which is faster than DP-ASV, may also be useful for this electrode.

REFERENCES

1. NAS 1977,*"Drinking water and health",* National Academy of Sciences, Printing and Publication Office: Washington, DC.

2. Fromm, K.M. 2013, "Barium bright and heavy", *Nature chemistry,* vol. 5, no. 2, pp. 146-146.

3. Łukasik-Głębocka, M., Sommerfeld, K., Hanć, A., Grzegorowski, A., Barałkiewicz, D., Gaca, M. & Zielińska-Psuja, B. 2014, "Barium Determination in Gastric Contents, Blood and Urine by Inductively Coupled Plasma Mass Spectrometry in the Case of Oral Barium Chloride Poisoning", *Journal of Analytical Toxicology,* vol. 38, no. 6, pp. 380-382.

4. Merefield, J.R. 1987, "Ten years of barium build-up in the Teign", *Marine Pollution Bulletin,* vol. 18, no. 5, pp. 220-222.

5. Spangenberg, J.V. & Cherr, G.N. 1996, "Developmental effects of barium exposure in a marine bivalve (Mytilus californianus)", Environmental Toxicology and Chemistry, vol. 15, no. 10, pp. 1769-1774.

6. Kravchenko, J., Darrah, T.H., Miller, R.K., Lyerly, H.K. & Vengosh, A. 2014, "A review of the health impacts of barium from natural and anthropogenic exposure", Environmental Geochemistry and Health, vol. 36, no. 4, pp. 797-814.

7. Environmental Protection Agency [US EPA] 2013, "Barium". Retrieved from http://www.epa.gov/ogwdw/pdfs/factsheets/ioc/tech/barium.pdf

8. Ghose, A., Sayeed, A. A., Hossain, A., Rahman, R., Faiz, A., & Haque, G. 2009, "Mass barium carbonate poisoning with fatal outcome, lessons learned: A case series". Cases Journal, 2(1), 9069-9069. doi:10.4076/1757-1626-2-9069

9. Koch, M., Appoloni, O., Haufroid, V., Vincent, J., & Lheureux, P. 2003, "Acute barium intoxication and hemodiafiltration". Clinical Toxicology, 41(4), 363-367. doi:10.1081/CLT-120022004

10. TOXNET 2014, "*Barium, Elemental",* Hazardous Substances Data Base [HSDB] Retrieved from http://toxnet.nlm.nih.gov/cgi-bin/sis/search2/f?./temp/~HBQQMC:1

11. NHMRC, NRMMC 2011, "*Australian Drinking Water Guidelines Paper 6 National Water Quality Management Strategy"*. National Health and Medical Research Council, National Resource Management Ministerial Council, Commonwealth of Australia, Canberra.

12. World Health Organisation [WHO] 2011, "*Guidelines for drinking water quality",* 4th ed. Retrieved from http://whqlibdoc.who.int/publications/2011/9789241548151_eng.pdf

13. Kato, M., Ohgami, N., Ly, T.B., Jia, X., Yetti, H., Naito, H. Nguyen D.T. 2013, "Comparison of barium and arsenic concentrations in well drinking water and in human body samples and a novel remediation system for these elements in well drinking water: E66681". *PLoS One, 8*(6) doi:10.1371/journal.pone.0066681

14. Yajima, I., Kato, M., Uemura, N., Nizam, S., Khalequzzaman, M., Thang, N. D., Nakajima, T. 2012, "Barium inhibits arsenic-mediated apoptotic cell death in human squamous cell carcinoma cells". *Archives of Toxicology, 86*(6), 961-973. doi:10.1007/s00204-012-0848-9

15. Wang, J., Farias, P.A.M. & Mahmoud, J.S. 1985, "Trace measurements of calcium, magnesium, strontium and barium, based on stripping voltammetry with adsorptive accumulation", *Journal of Electroanalytical Chemistry,* vol. 195, no. 1, pp. 165-173.

16. Salaün, P., Gibbon-Walsh, K. & van den Berg, C. M. G. 2011, "Beyond the hydrogen wave: New frontier in the detection of trace elements by stripping voltammetry". *Analytical Chemistry, 83*(10), 3848. doi:10.1021/ac200314q

17. Kelly, R.S. 2009a, "Anodic Stripping Voltammetry" page in Analytical Chemistry: The Basic Concepts, e-courseware, Analytical Sciences Digital Library [ASDL]. Retrieved from http://www.asdlib.org/onlineArticles/ecourseware/Kelly_Potentiometry/PDF-13-ASV.pdf 27.3.15

18. Woolever, C.A. & Dewald, H.D. 2001a, "Differential pulse anodic stripping voltammetry of barium and lead in gunshot residues", *Forensic Science International,* vol. 117, no. 3, pp. 185-190.

19. O'Mahony, A.M. & Wang, J. 2013, "Electrochemical Detection of Gunshot Residue for Forensic Analysis: A Review", *Electroanalysis,* vol. 25, no. 6, pp. 1341.

20. Bard, A.J., Parsons, R. & Jordan, J. Eds.1985, *Standard Potentials in Aqueous Solution,* Marcel Dekker, Inc, New York.

21. Kovaleva, S.V, Gladyshev, V.P & Chikineva, N.V 2001, "Determination of Barium by Stripping Voltammetry", *Journal of Analytical Chemistry,* vol. 56, no. 5, pp. 449-449.

22. Woolever, C.A. & Dewald, H.D. 2001b, "Stripping Voltammetry of Barium Ion in the Presence of Lead", *Electroanalysis,* vol. 13, no. 4, pp. 309-312.

23. Wajrak, M. 2009, "Modern Water Report".

24. Heineman, W.R. & Kissinger, P.T. 1996, *Laboratory techniques in electroanalytical chemistry,* Marcel Dekker, Inc, New York.

25. Chan, D. & Stachowiak, G.W. 2004, "Review of automotive brake friction materials", *Proceedings of the Institution of Mechanical Engineers, Part D: Journal of Automobile Engineering,* vol. 218, no. 9, pp. 953-966.

26. Wang, J. 2005, "Stripping Analysis at Bismuth Electrodes: A Review", *Electroanalysis,* vol. 17, no. 15-16, pp. 1341-1346.

27. Kelly, R.S. 2009b, "Working electrodes" page in Analytical Chemistry: The Basic Concepts, e-courseware, Analytical Sciences Digital Library [ASDL]. Retrieved from http://www.asdlib.org/onlineArticles/ecourseware/Kelly_Potentiometry/PDF-16-WorkingElec.pdf 27.3.15

28. Agrawal, J.K., Sharma, J.D. & Pitre, K.S. 2005, "Differential Pulse Anodic Stripping Voltammetric Analysis of Firearm Discharge Residues", *IndMedica,* vol. 5, no. 4, pp. 5.

29. Lu, M., Rees, N.V. & Compton, R.G. 2012, "Determination of Sb(V) using differential pulse anodic stripping voltammetry at an unmodified edge plane pyrolytic graphite electrode", vol. 24, no. 6, pp. 1306-1310.

30. Vuki, M., Shiu, K., Galik, M., O'Mahony, A.M. & Wang, J. 2012, "Simultaneous electrochemical measurement of metal and organic propellant constituents of gunshot residues", *The Analyst,* vol. 137, no. 14, pp. 3265-327.

31. Centre for Disease Control [CDC] 2009, "Surface sampling procedures for heavy metals" page. National Institute for Safety and Health, USA. Retrieved from http://www.cdc.gov/niosh/docs/2009-133/pdfs/DREAM2008-SurfaceBio-Ashley1-NIOSH.pdf

32. Collins, P., Coumbaros, J., Horsley, G., Lynch, B., Kirkbride, K.P., Skinner, W. & Klass, G. 2003, "Glass-containing gunshot residue particles: a new type of highly characteristic particle?", *Journal of Forensic Sciences,* vol. 48, no. 3, pp. 538.

33. Anson, F. C. 1975, "Patterns of ionic and molecular adsorption at electrodes." *Accounts of Chemical Research, 8*(12), 400-407. doi:10.1021/ar50096a002.

34. Compton, R. 2007, *Understanding Voltammetry.* Singapore: World Scientific Publishing Co. Pte. Ltd.

35. Wu, H. P. 1996, "Dynamics and Performance of Fast Linear Scan Anodic Stripping Voltammetry of Cd, Pb, and Cu Using In Situ-Generated Ultrathin Mercury Films", *Analytical Chemistry 68*(9), 1639-1645.

36. Tufa, L.T., Siraj, K. & Soreta, T. R. 2013, "Electrochemical determination of lead using bismuth modified glassy carbon electrode", *Russian Journal of Electrochemistry, 49*(1), 64-72.

37. Princeton Applied Research. n.d., *Fundamentals of Stripping Voltammetry (Application Note S-6)*. Retrieved from http://www.princetonappliedresearch.com/Literature/index.aspx

38. Water Corporation. 2012, "Drinking Water Quality, Annual Report 2011/2012". Retrieved from http://www.watercorporation.com.au/~/media/files/about-us/our-performance/drinking-water-quality/annual-report-2012.pdf

39. Garofano, L., Capra, M., Ferrari, F., Bizzaro, G.P., Di Tullio, D., Dell'Olio, M. & Ghitti, A. 1999, "Gunshot residue. Further studies on particles of environmental and occupational origin", *Forensic Science International 103* 1-21.

40. Opoka, W., Jakubowska, M., Baś, B., & Sowa-Kućma, M. 2011, "Development and validation of an anodic stripping voltammetric method for determination of Zn2+ ions in brain microdialysate samples". *Biological Trace Element Research, 142*(3), 671-682.

41. Modern Water, 2011, *PDV6000plus Application Notes,* Unit 15 – 17 Cambridge Science Park, Milton Road, Cambridge, CB4 0FQ, United Kingdom.

42. Gietl, J. K., Lawrence, R., Thorpe, A. J., & Harrison, R. M. 2010, "Identification of brake wear particles and derivation of a quantitative tracer for brake dust at a major road". *Atmospheric Environment, 44*(2), 141-146.

APPENDIX

Table 12. Linear Sweep potential delivery, GCE, 0.05M KCl + Hg 5ppm electrolyte solution, 60 sec deposition time (t_{dep}), deposition potential (dp) = -3.000V, Ba 50ppb + Pb 50ppb, altering the scan rate for investigation of peak height and optimal speed.

Scan rate (mV/s)	Ba peak (μA)	Pb peak (μA)
50	-	2.92
100	-	2.89
200	2.55	5.84
400	7.52	11.85
500	15.26	16.60
600	7.77	20.73
800	9.27	30.73
1000	16.17	41.54
1600	20.43	66.69
3200	23.05	104.80

Table 13. Differential Pulse potential delivery, GCE, 0.05M KCl + Hg 5ppm electrolyte solution, 60 sec deposition time (t_{dep}), deposition potential (dp) = -2.500V, Ba 50ppb + Pb 50ppb, altering the scan rate for investigation of peak height and optimal speed.

Scan rate (mV/s)	Ba peak (μA)	Pb peak (μA)
10	35.47	221.2
20	51.99	198.9
50	80.42	229.35
100	71.15	144.15
150	32.01	83.23
200	-	16.03
300	-	-
500	5.92	1.16

Table 14. Peak heights for change in deposition time at deposition potentials ranging from -3000V – -2400V, Ba 10ppb, 0.05M KCl, differential pulse, 100mV/s.

Deposition Potential (V)	Deposition Time (sec)							
	Ba peak (μA)				Pb peak (μA)			
	10	30	60	120	10	30	60	120
-3000	2.04	3.08	8.13	21.19	6.97	15.54	27.67	42.19
-2900	-	4.51	6.31	12.84	9.97	19.20	29.43	40.73
-2800	-	6.29	11.77	20.40	6.35	13.90	23.83	42.32
-2700	-	9.34	19.65	34.55	7.03	17.47	33.89	55.20
-2600	5.19	21.07	24.57	37.08	4.23	16.66	34.13	72.73
-2500	9.02	37.97	51.6	101.9	8.01	32.93	66.72	111.0
-2400	11.0	39.22	78.16	103.30	11.51	39.61	83.62	131.20

Table 15. Barium concentrations found in 10 drinking water samples in Perth, WA using voltammetric analysis.

	Barium (ppb)								
Sample	Trial 1	r^2	Trial 2	r^2	Trial 3	r^2	Mean	Std. dev.	%RSD
1	71.26	0.999	40.11	0.999	114.3	0.999	75.22	±37.25	49.5
2	8.76	0.999	7.05	0.999	9.59	0.999	8.47	±1.29	15.23
3	441.1	0.999	381.1	0.999	411.4	0.999	411.2	±30.0	7.29
4	434.2	0.999	489.8	0.999	469.7	0.999	464.56	±28.15	6.1
5	73.27	0.999	72.82	0.999	75.73	0.999	73.94	1.57	2.1
6	40.12	0.999	55.91	0.999	50.19	0.999	48.74	±7.99	16.4
7	446.3	0.999	399.3	0.999	443.6	0.999	429.73	±26.39	6.1
8	423.5	0.999	414.9	0.999	420.9	0.999	419.76	±4.41	1.1
9	56.2	0.999	58.13	0.999	68.35	0.999	60.89	±6.53	10.72
10	7.618	0.997	7.477	0.999	7.676	0.992	7.59	±0.10	1.3

Table 16. Barium concentrations found in 5 brake pad dust samples in Perth, WA using voltammetric analysis.

Brake pads	Barium concentration (ppm)								
Sample	Trial 1	r^2	Trial 2	r^2	Trial 3	r^2	Mean	Std. dev.	%RSD
12	14.46	0.999	7.91	0.999	13.03	0.999	11.78	3.42	29.0
13	8.48	0.999	9.05	0.999	8.16	0.999	8.56	0.45	5.3
14	1.65	0.999	1.52	0.999	1.84	0.999	1.67	0.16	9.6
15	2.83	0.999	2.42	0.999	2.39	0.999	2.54	0.24	9.4
16	4.95	0.999	4.91	0.999	4.72	0.999	4.86	0.12	2.5